RESEARCH PAPER

Modeling the Dynamic Recrystallization by Using Cellular Automaton: The Current Status, Challenges and Future Prospects

M. Azarbarmas*

** azarbarmas@sut.ac.ir*

Received: September 2019 **Revised: February 2020** **Accepted: April 2020**

* Research Center for Advance Materials, Faculty of Materials Engineering, Sahand University of Technology, Tabriz, Iran

DOI: 10.22068/ijmse.17.4.103

Abstract: *Mechanical properties of metals are substantially dependent on the microstructure, which can be controlled by thermo-mechanical parameters such as temperature, strain, and strain rate. Hence, understanding the microstructural evolution of alloys during the hot deformation is crucial to engineer the metal forming processes. The main objective of this work is to present an overview of cellular automaton (CA) modeling to predictthe microstructure of alloys experienced the dynamic recrystallization (DRX) phenomenon. In this review paper, first, overall descriptions about the DRX phenomenon and the CA modeling are presented. Then, the CA modeling procedure is compared with similar methods. Meanwhile, related studies in the field of the DRX simulation by using the CA modeling are evaluated. Four main stages of the CA modeling are analyzed in terms of the "nucleation", "growth", "topological changes" and "texture evaluation" steps. Most important limitations including the calibration sensitivity, limitations in modeling the continuous DRX, ignoring microstructural effects on the deformation behavior, limited applications, and limited database as well as the saturation in published works are discussed and then objective suggestions are presented to overcome these limitations. Finally, prospects in the CA modeling of DRX are provided in the last section.*

Keywords: *Dynamic recrystallization, Modeling, Cellular automaton, Microstructure.*

1. INTRODUCTION

It is well established that the microstructure controls the physical and mechanical properties of polycrystals. The microstructure controlling is an interesting branch of both industrial and scientific researches. Among microstructural developments, DRX is a well-established mechanism for grain refinement under the hot plastic deformation [1, 2]. In the past decades, modeling and predicting the microstructure have gained extensive attention worldwide and several numerical techniques such as Monte Carlo (MC), vertex, phase field, and CA models have been successfully used to model the microstructure during the hot deformation. In comparison with alternative modeling procedures, the CA modeling is more feasible to simulate the microstructural evolution and topology features [3]. In the CA modeling, the first step is recognizing the main features of the phenomenon and defining them in a suitable form to obtain a numerical model [4]. Although most of the theoretical works based on CA modeling have been limited to mathematics and computer science [5], CA has been utilized by various researchers in materials science and engineering to model static recrystallization (SRX) [6-12], DRX [13,14], solidification of metals [15-17], nitriding [18], corrosion behavior [19-21], growth [22-24], predicting the cracking [25-28] and phase transformations [29-31] of various alloys. Table 1 presents a list of works published in the field of DRX modeling by using the CA method. It can be seen that scientists have become increasingly intrigued by the idea of DRX modeling utilizing CA in recent years.

The approach proposed by Goetz and Seetharaman [32] can be considered as the first CA modeling for the DRX phenomenon under isothermal and constant strain rate conditions. A large number of works published in this field have very simple assumptions such as assigning a scaler number for grain orientation (0-180) [33,34], modeling the deformation without changing in the shape [35,36] and orientation of grains [37,38], neglecting the precipitation effects [39,40] and ignoring the features that distinguish between the high and low angle grain boundaries [41,42].

Table 1. Published works in the field of CA modeling of the DRX process.

Reference	Year	Coupled module	Reference	Year	Coupled module
R.L. Goetz V. Seetharaman [32]	1998	-	E.Popova et al. [49]	2015	Crystal plasticity
G. Kugler R. Turk [135]	2004	-	M. Sitko et al. [136]	2015	
M. Qian, Z.X. Guo [34]	2004	-	P. Asadi et al. [137]	2015	
J. Gawąd, M. Pietrzyk [127]	2007	Continuum macroscale simulation via FEM	X.H. Deng et al. [138]	2015	
N. Yazdipour et al. [139]	2007	-	M. Sitko et al. [140]	2015	Finite Element model
N. Xiao et al. [33]	2008	Uniform topology	E. Popova [52]	2015	Crystal plasticity finite element method
N. Yazdipour et al. [111]	2008	-	J. De Jaeger et al. [54]	2015	Crystal plasticity model
J.W. Zhao et al. [41]	2008	-	H. Li et al. [53]	2016	Crystal plasticity framework
H. Shi-quan et al. [112]	2009	-	F. Han et al. [141]	2016	-
H. W. Lee, Y. Taek Im [42]	2010	-	J. Haipeng et al. [142]	2016	-
H. W. Lee Y. T. Im [35]	2010	-	L. Jun-chao et al. [44]	2016	Uniform topology
H. Hallberg et al. [62]	2010	-	F. Chen [45]	2016	Uniform topology
J. Zhao-yang et al. [143]	2010	Adaptive response surface method as optimization model	C. Zhang [114]	2016	-
Z. Jin, Z. Cui [119]	2012	-	M. Sitko et al. [46]	2016	Uniform topology
W. Chuan et al. [51]	2013	Crystal plasticity finite element method	P. Asadi et al. [122]	2016	Laasraoui-Jonas models
Y. Zhang et al. [116]	2013	-	F. Chen et al. [47]	2016	Uniform topology
X. Liu et al. [38]	2013	-	M. Akbari et al. [144]	2016	Finite element model
F. Chen et al. [43]	2014	Uniform topology	H.P. Ji et al. [145]	2016	
H. Shi-quan et al. [146]	2014	-	Y. Wang et al. [147]	2016	Finite element method
A. Timoshenkov et al.[125]	2014	Module for retarding effect of precipitates	M. Sitko and Ł. Madej [148]	2016	Finite element method
Y.X. Liu et al.[109]	2015	-	A. Legwand et al. [149]	2016	Finite element method
X. Ma et al.[150]	2016	Uniform topology	M. Azarbarmas et al. [108]	2018	Phenomenological Approach
Y.X. Liu et al.[96]	2017	-	L. Madej et al. [151]	2018	Finite element model
X. Li et al.[152]	2017	Finite element software, DEFORM-3D	Q. Xu et al. [153]	2018	-
X.J. Guan [154]	2017	-	Y.N. Guo et al. [155]	2018	Optimized topology deformation technology
Y.P. Lou et al.[156]	2017	-	C. Duan et al. [157]	2018	Finite element
Z. Wang et al.[158]	2017		L. Li et al.[159]	2018	-
M. S. Chen [160]	2017	-	S.Y. Yang et al.[161]	2018	-
Y.X. Liu et al. [96]	2017	-	G.Z. Quan et al. [162]	2018	Cellular automaton calculation for dynamic recrystallization
M. Azarbarmas and M. Aghaie-Khafri [97]	2017	Uniform topology-Sachs model	Z.H Cao et al. [163]	2019	-
T. Zhang et al.[164]	2017	-	H. Zhang et al. [165]	2019	-
W. Xu et al. [166]	2017	-	F. Zhang et al. [115]	2019	
M.S.Chen et al. [167]	2017	-	J. Zhang et al. [168]	2019	-
L.Wang et al. [169]	2018	-	C. Zhang et al. [170]	2019	-
L.Wang et al. [169]	2018	-	Y. Wang et al. [171]	2019	-
A. Samanta et al. [172]	2018	-	C. Wu et al.[173]	2019	Finite element model
F. Chen et al. [174]	2018		F. Sun et al.[175]	2019	A fingerprint image enhancement algorithm to generate real initial microstructure
M. Azarbarmas and M. Aghaie- Khafri [50]	2018	Rate-dependent model	D.D. Chen et al. [134]	2019	Neural network-based model predictive control

From the literature review, it can be found that most of the latest published works are to overcome the aforementioned simplifications. N. Xiao et al. [33] and then other researchers [43-47] used a uniform topology module for tracking the changes in grains shape during the deformation. On the other hand, using the actual orientation for grains in terms of Euler angles [48] or the rotation matrix [49] is another development in the CA modeling of DRX.

One of the main characteristics of CA modeling is its ability to couple with other models to improve its performance. Recently, Azarbarmas and Aghaie-Khafri [50] have published a work in which the CA model has been coupled with a rate-dependent model to trace the orientation changing during the hot deformation. Also, Chuan et al. [51] and other authors [52-53] have utilized the CA modeling coupled with the crystal plasticity finite element method for increasing the CA accuracy in predicting the microstructural developments during the DRX phenomenon.

Extension of recrystallized microstructures modeling from two to three-dimensional domain is another interesting issue in this field. Li et al. [53] and Jaeger et al. [54] have developed the CA model for predicting the DRX behavior of Ti alloy and Ni alloy, respectively, during the hot compression test. Although these models need more time and calculations, they can present the results in a three-dimensional space.

Although there are many published works in the field of DRX modeling based on CA (see Table 1), none of them have focused on the advantages, limitations, and future prospects of this method and there is no comprehensive work reviewing the published works about the DRX modeling by using the CA approach. One of the unique features of this work is providing a critical evaluation of the CA modeling in microstructural modeling. Most of the works published in this field have only focused on the advantages of this method without considering the limitations of it. Another important part of this study is presented as "future prospects", which inspires a promising route for researchers to use CA modeling for scientific and industrial developments in the future. This paper provides a summary of the CA modeling of the DRX process in metals and alloys. In the following sections, after introducing the CA algorithm, it is compared with other microstructural modeling methods followed by a detailed description of CA steps including the "nucleation", "growth" and "topological and texture evolution" stages. Finally, several challenges, corresponding recommendations, and future prospects are listed.

Table 2. Nomenclature

B	Burgers vector	T	The temperature
C	constant	u	The vector in the deformed position
dE	The energy change	U*	The stretch tensor
dE_S	Surface energy changes	V	The boundary velocity
dE_υ	Volume energy changes	v	The vector in the undeformed position
F*	The non-plastic deformation gradient	α	The dislocation-interaction coefficient
H	The work hardening term	Γ	The energy of grain boundaries
I_x, I_y	The nominal deformation at two principal directions	γ_m	The energy of high angle grain boundaries
K_1	A constant showing the effect of the work hardening	ε	The strain
K_2	A constant showing the effect of the softening	$\dot{\varepsilon}$	The strain rate
M	The mobility of grain boundaries	η	The percentage of DRX measured experimentally
M_m	The mobility of a high angle boundary	θ	The misorientation of a grain boundary
$\dot{n}$	The nucleation rate	Θ_0	The work hardening rate
Q	The nucleation activation energy	θ_m	The misorientation of a high angle grain boundary
Q_R	The rotation tensor	M	Shear modulus
R	Gas constant	ρ	The dislocation density
r	The dynamic recovery term	σ_S	The steady-state stress
R*	The rigid rotation of the material lattice	τ	The dislocation line energy
r_d	The mean radius of DRX grains	υ_p	Poisson ratio
S	The deformation matrix		

2. DYNAMIC RECRYSTALLIZATION

The final microstructure and mechanical properties of metals can be controlled by the recrystallization and related phenomena. In the case of alloys with low stacking fault energy, DRX takes place readily during the hot deformation [55] due to the limited dynamic recovery, resulting in flow curves having peak stress [56,57]. Recently, Huang and Logé [58] have provided an integrated overview of DRX in metallic materials. Two main types of DRX mechanisms are the discontinuous DRX (DDRX) and continuous DRX (CDRX) [59]. Additionally, the geometric DRX (GDRX) can also occur in presence of large strains and elevated temperatures. During the GDRX phenomenon, older grains are elongated with local serrations which can convert to equiaxed grains with high angle grain boundaries (HAGBs) as a result of more grain thinning. The schematic representation of these three types of DRX is exhibited in Fig. 1.

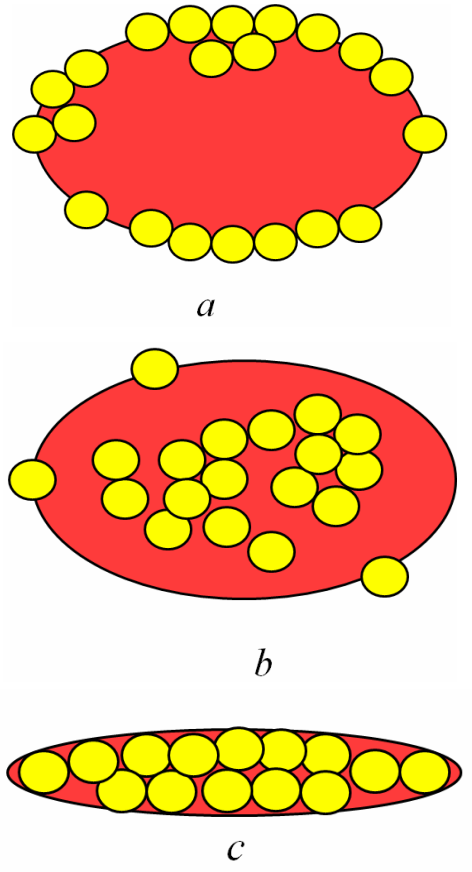

Fig. 1. The schematic presentation of three types of DRX; a) DDRX, b) CDRX and c) GDRX.

Typical DRX flow curves are serrated stress-strain curves with single or multi-peak oscillations due to the competition between the work hardening and the softening. As seen in Fig. 2, the plastic area of curves comprises three parts: The first is the work hardening stage in which the dislocation density gradually increases, and thereby the flow stress increases with increasing the strain. The second one is the softening stage; because the dislocation density has reached a critical value, DRX takes place and so the density of dislocations is decreased [60]. The last stage of flow curves is the steady-state, in which a balance between the work hardening and softening processes is attained. The overall shape of a flow curve is completely affected by microstructural changes. Flow curves of CDRX experienced alloys have multiple peaks [61]. It is due to this fact that recrystallization cycles are not synchronized, against the DDRX mechanism having a single peak flow curve, Fig. 2.

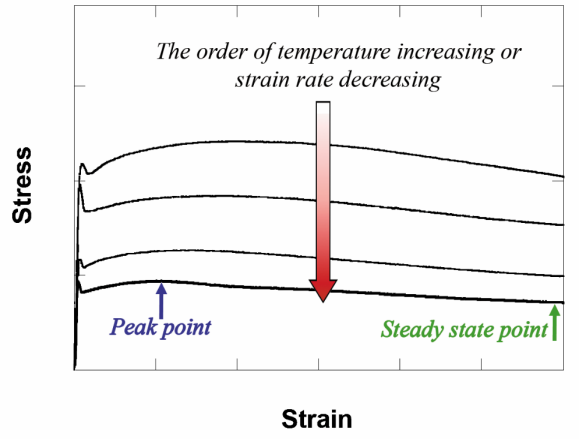

Fig. 2. Schematic flow stress curves showing the typical form of DRX experienced flow curves.

2.1. Discontinuous Dynamic Recrystallization

The DDRX process, known as the conventional DRX, is characterized by clear nucleation and growth steps. DDRX often takes place during the hot deformation of metals and alloys with low or medium stacking fault energy. Pre-existing grain boundaries with sufficient stored energy are the preferred nucleation sites in DDRX, owing to the serrated and barreled area and the subsequent strain-induced boundary migration [62]. This is why that a necklace structure is a common feature of DDRX, see Fig. 3 in which the microstructure of Inconel 718 superalloy

reported by the author of this work and Aghaie-Khafri [50] is presented. It is well known that after reaching the steady-state condition a saturation size of recrystallized grains is obtained in each condition of the deformation temperature and strain rate. A relationship between the Zener-Hollemon parameter and the steady-state DRX grain size can be found.

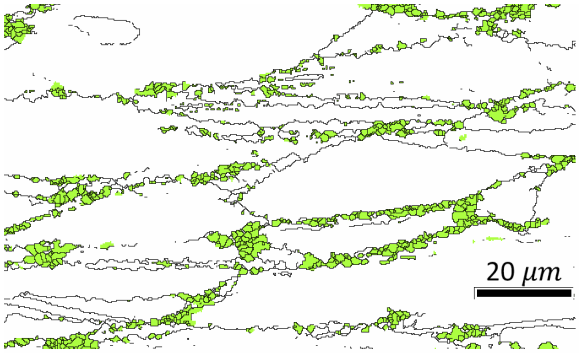

Fig. 3. An orientation imaging microscopy (OIM) image showing the necklace-type microstructure of the hot compressed nickel-based superalloy, indicating the occurrence of DDRX [50].

One of the main features of DDRX is a flow stress curve with a single peak [63], Fig. 2, indicating that new cycles of DRX onset before the completion of current cycles [64]. It means that each grain is at a different stage of the DRX development during the deformation. In other words, the appeared single peak flow curve is the equilibrium flow stress of all grains at various states of DRX.

2.2. Continuous Dynamic Recrystallization

Metals and alloys having high stacking-fault energy show the intense dynamic recovery. So, CDRX will be the dominating DRX mechanism during the hot deformation of these alloys [65]. Because the dynamic recovery is so fast, dislocation density differences across grain boundaries are not discernible. Accordingly, there is no sufficient driving force for the dynamic grain boundary migration required for the DDRX mechanism. CDRX, which is also called the "apparent DRX" or "extended dynamic recovery" [66], is commonly known by the dislocation cell boundary formation, transforming to low angle grain boundaries (LAGBs) and then to HAGBs [67,68]. Therefore, CDRX is not a mechanism controlled by nucleation and growth. This is why that recrystallized grains via the CDRX mechanism are finer and more uniform, having a grain size equal to the size of cell boundaries. One of the microstructures experienced CDRX is shown in Fig. 4. It can be seen that both the cumulative misorientation (point to the origin) and the local misorientation (point to point) along grain interior parts have high values indicating the progressive subgrain rotation inside original grains.

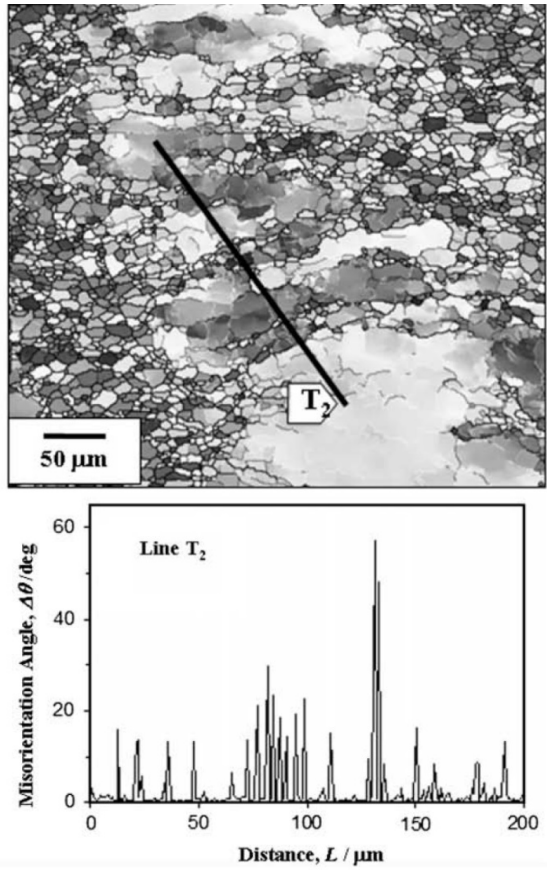

Fig. 4. An OIM micrograph and the corresponding misorientation profile for AA7475 alloy deformed at the strain rate of 3×10^{4} s $^{-1}$ [69].

3. CELLULAR AUTOMATON METHOD

The CA modeling of the recrystallization is the preferred method when the capillary driving force is negligible compared to the driving force due to the stored elastic energy [70]. In two and three-dimensional representations of a CA model, an interface between two grains can be illustrated by lines and surfaces which are approximated within the CA grid. The simplest and common form of cells is in a periodic grid of squares in two-dimensional or cubes in three-dimensional. Other used grids in the CA modeling are exhibited in Fig. 5.

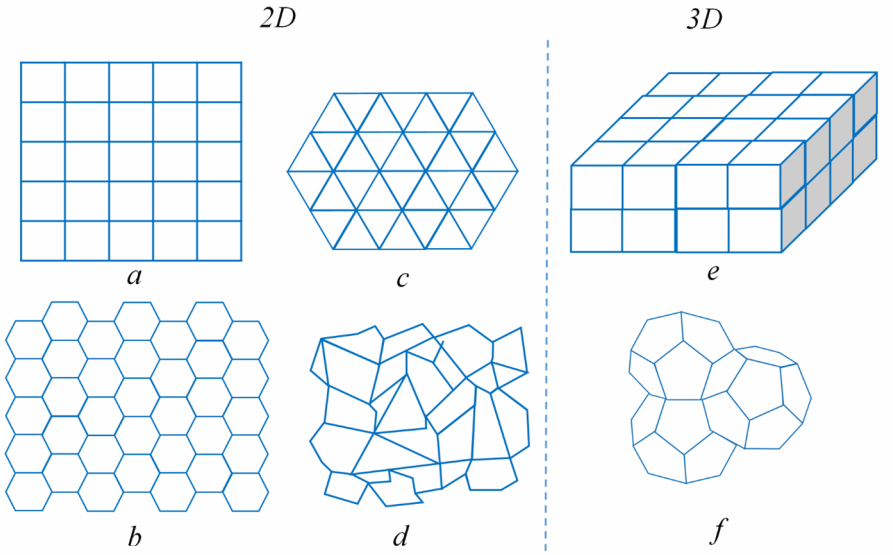

Fig. 5. a) The square, b) triangle, c) hexagon, d) irregular distribution, e) cube and f) tetrakaidecahedron grids used in the CA modeling.

The most known neighborhood definitions are the von Neumann, Moore, and extended Moore in a two-dimensional square net of cells [71], though a 7-cells neighborhood can be also considered [72], Fig. 6. The required information regarding the state variables and neighboring definitions are assigned to each cell, Fig. 7. Transition rules define the status of a position as a function of its previous state and the state of neighboring sites (local rules) [73,74] or the state of all sites (global rules) [75], the former is common in most classical CA models. Transition rules can be considered as deterministic or stochastic, and updates are applied as synchronous or asynchronous [76]. The number, arrangement, and range of neighbor sites utilized by transformation rules determine the range of the interaction and the local shape of the evolving area [77,78]. The definition of a neighborhood can be modified by introducing a weighted neighborhood, i.e. the effects of a neighbor on other cells are considered with a weight, depending for example on the distance separating them from each other [79].

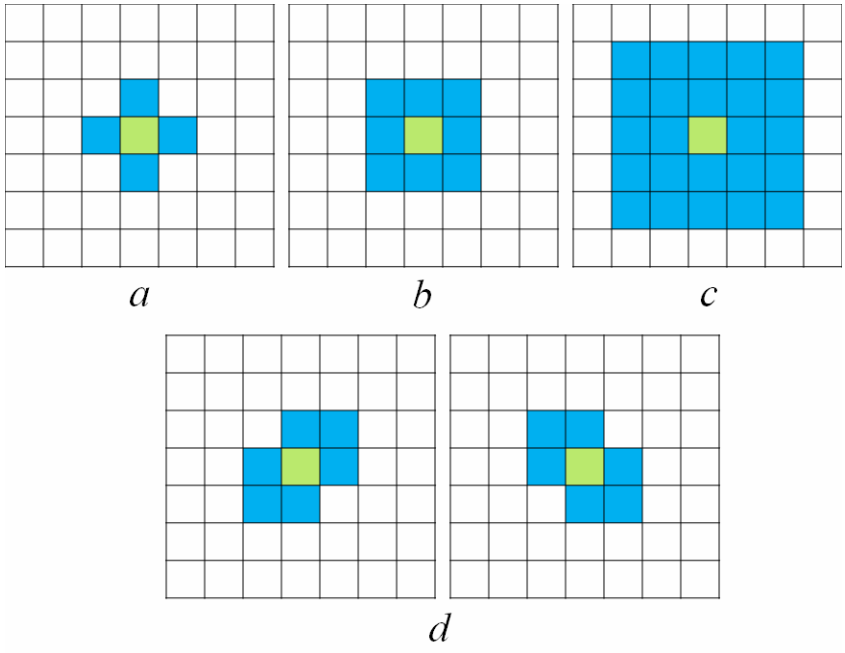

Fig. 6. Classic neighborhood definitions in the CA method.

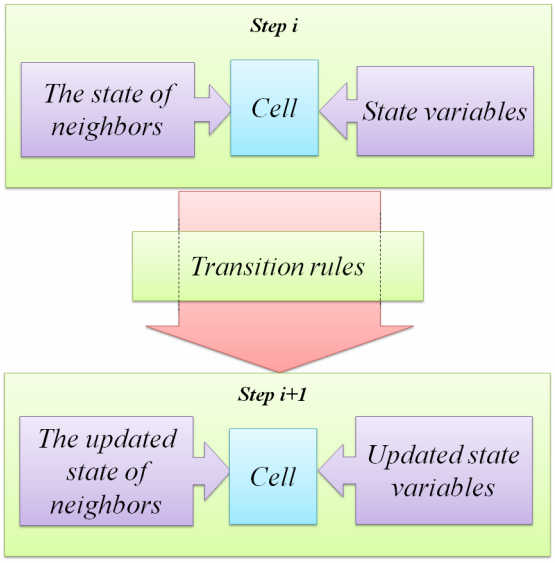

Fig. 7. The schematic showing parameters affecting the state of a cell; transition rules define the status of a cell as a function of its previous state and the state of the neighbors.

The most important variables defining the state of each cell are:

- The grain orientation which is used to separate different grains [8], and calculate the grain boundary energy and mobility [80],
- The dislocation density showing the strain stored energy [81],
- A parameter indicating the recrystallization state of cells [82],
- The grain boundary sign indicating the location of grain boundary cells [83].

4. COMPACTING CA WITH SIMILAR METHODS

Up to now, various numerical simulation methods such as MC [84-86], phase-field [87-91], vertex [92-94], and CA [95-96] models have been presented to perform the numerical modeling of the recrystallization evolution on the mesoscale. In addition to the high accuracy of the prediction, the procedure of the microstructural evolution can be visibly reproduced by using these models. In comparison with alternative modeling methods, the CA method is more feasible to model the microstructure owing to its intrinsic advantages of the calibration to the time and length scale [97, 98].

The MC method carries out an operation at each site in each time step, while the CA model performs only at sites with the potential of participating in the transformation. Consequently, MC modeling is computationally intensive in comparison with CA modeling [99]. Also, the MC model utilizes arbitrary units and the basic criterion is the energy minimization, while the CA modeling uses physical units and it works considering analytical equations [100]. In other words, CA models do time integration by utilizing the physical time, whereas this is impossible in MC algorithms in which "MC steps" are used as a measure of the real-time [101].

The phase-field modeling is utilized for assessing the evolution kinetics of microstructural phenomena on the base of the comprehensive action of the thermodynamical driving force. Due to its heavy calculations, the phase-field method is more time-consuming than others. Similarly, the use of vertex models has been gradually limited, because it needs a complex calculation of the vertex driving force and determination of vertex equations.

The CA approach provides precisely tracking the recrystallization front, and modeling steps are limited to real-time based on analytical equations. All of the listed facts indicate that the CA method is more attractive in practice.

5. MAIN STAGES OF THE CA MODELING

5.1. CA Modeling of the Nucleation

The CA modeling the recrystallization is based on the idea that the recrystallization can be considered as a simple change of the state, i.e. from the deformed to the recrystallized state [48]. To model DRX, two main steps are executed which are inevitably considered in all CA algorithms, see Fig. 8:

- The first stage regards the formation of nuclei inside the deformed area.
- The second stage is the subsequent growth of nuclei into deformed grains.

As soon as a defined state variable of a cell reaches the critical value, the DRX nucleation occurs on the cell and the state variable of it changes from the un-recrystallized to the recrystallized state according to switching rules. In the nucleation step, nuclei with a given radius are arranged within the grid. The employment of nuclei as spheres is crucial to overcome the effects of the grid geometry on grain geometry

[102]. The dislocation density [34, 35] or the stored strain energy [54] of cells can be used as the controlling state variable. The critical dislocation density is obtained by utilizing some equations while the critical stored energy can be implemented as an arbitrarily fixed value [54].

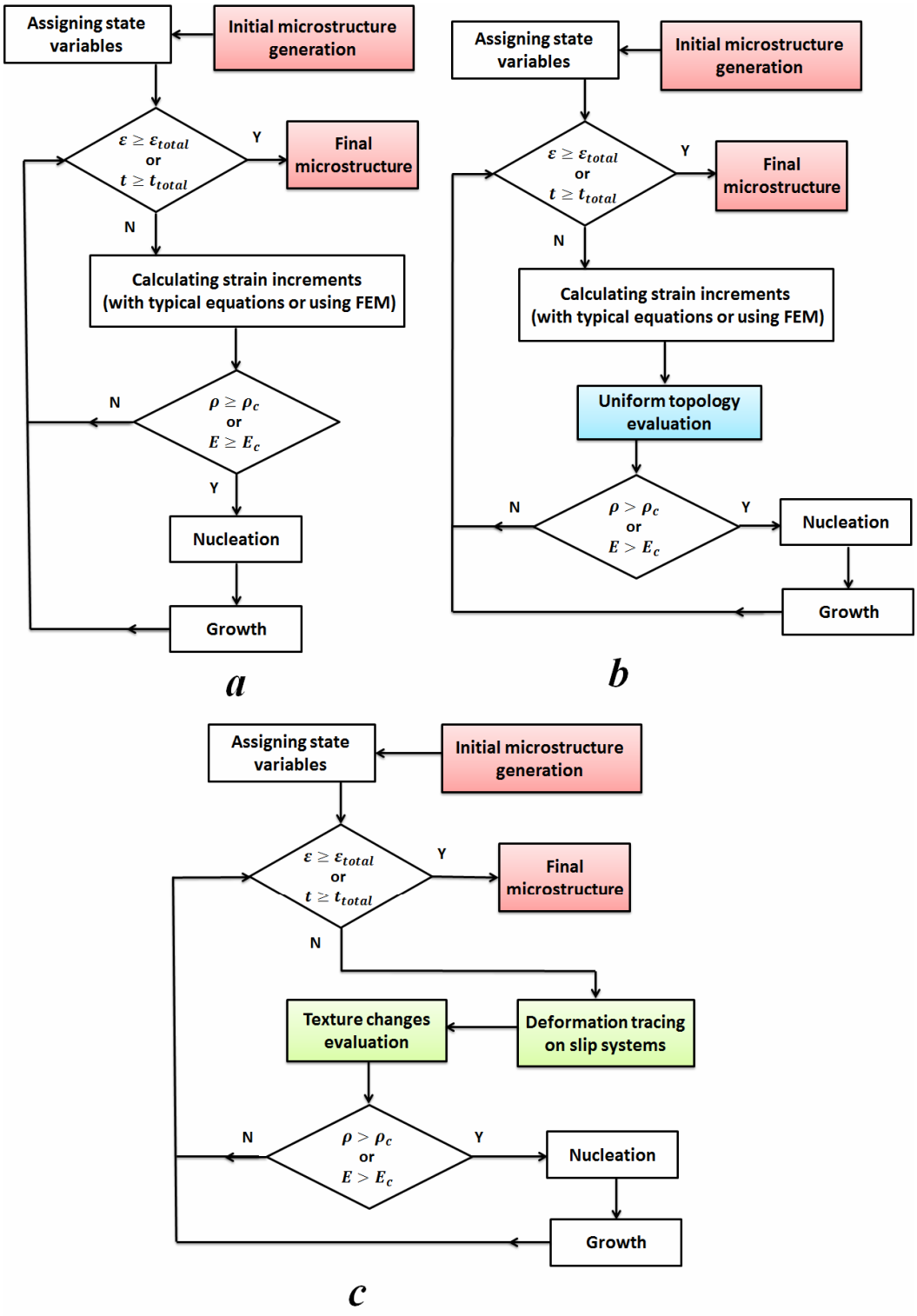

Fig. 8. Overall CA algorithms (a) in the classic form, (b) with the topological evaluation and (c) coupled with CPFEM.

The dislocation density evolution is governed by the dislocation multiplication and annihilation during the deformation. Kocks and Mecking [103] have proposed a phenomenological method to estimate the variation of the dislocation density with strain increments, equation (1). Yoshie–Lassraoui–Jonas's model can be also used to evaluate the dislocation density as $d\rho=(h-r\rho)d\varepsilon$ [40], where h and r denote the work hardening and dynamic recovery terms, respectively.

$$\frac{d\rho}{d\varepsilon} = K_1\sqrt{\rho} - K_2\rho \quad (1)$$

Where K_1 is the hardening coefficient, and K_2 is the softening coefficient. The coefficients, K_1 and K_2, can be expressed as [104]:

$$K_1 = \frac{2\theta_0}{\alpha\mu b} \quad (2)$$

$$K_2 = \frac{2\theta_0}{\sigma_S}$$

where θ_0 is the initial hardening rate determined from the slope of the experimental stress-strain curve in the work hardening stage at a given temperature [105], α is the dislocation-interaction coefficient (between 0.5 and 1.0 for most alloys), μ denotes the shear modulus, b indicates the Burgers vector and σ_S is the steady-state stress.

It should be pointed out that only cells located along grain boundaries are considered as preferred nucleation sites which are randomly selected. This satisfies conditions for the DDRX process which is a two-step process comprising the nucleation and growth of strain-free grains [106]. This mechanism will result in the formation of a necklace structure [107]. Because of the simplicity of the nuclei distributing along the initial grains, most of the CA-based studies have focused on alloys that show the necklace structure during the DRX process, see Fig. 9. However, some limited works have been reported to model the CDRX mechanism by using the CA method. Lately, the author of this work et al. [108] have presented a combined method based on the CA modeling and a phenomenological approach for modeling the CDRX phenomenon. This model was intrinsically a DDRX predicting model which has been accommodated to the CDRX condition. The main transition rules of this model can be summarized as 1) the nucleated DRX grains were distributed inside the initial grains, not only along the primary grain boundaries and 2) the recrystallization was modeled as a one-step process without any large-scale growth, which is the characteristic of the CDRX phenomenon.

In CA models, it is assumed that nuclei appear continuously at a constant rate [109]. The rate of the nucleation per unit of the grain boundary area is defined as a function of the strain rate and the deformation temperature [110]:

$$\dot{n} = C\dot{\varepsilon}\left(-\frac{Q}{RT}\right) \quad (3)$$

Where C is a temperature-dependent parameter and Q is the activation energy of the nucleation Zhang et al. [116] have used $\dot{n} = \frac{\dot{\varepsilon}}{\varepsilon}\frac{3\eta}{4\pi r_{d^3}}$ equation to determine the nucleation rate; η is the percentage of the recrystallized area measured experimentally for a specific deformation condition, and rd is the mean radius of DRX grains. The stored and released energy [98, 12, 105, 106], or the dislocation density [119] can also be a factor to determine the nucleation rate.

5.2. CA Modeling of the Growth

New DRX nuclei grow by consuming the strain-hardened older grains. The driving force for the growth of nuclei is originated from the change of energy. The energy change can be divided into volume and surface energy changes. For a spherical grain:

$$dE = dE_\upsilon + dE_S = \frac{4\pi}{3} r_{d^3}\tau\Delta\rho - 4\pi r_{d^2}\gamma \quad (4)$$

where τ is the dislocation line energy, which is expressed as $\tau=0.5\mu b^2$ [120], Δρ is the difference of the dislocation density between growing DRX grains and their neighboring grains, and γ is the surface energy of grain boundaries which can be determined by the Read–Shockley equation [121].

$$\gamma = \begin{cases} \gamma_m & \theta \geq 15^\circ \\ \gamma_m\left(\frac{\theta}{\theta_m}\left[1-\ln\left(\frac{\theta}{\theta_m}\right)\right]\right) & \theta < 15^\circ \end{cases} \quad (5)$$

Where θ_m is the critical misorientation for HAGBs, which is usually taken as 15˚, and γ_m is the surface energy of HAGBs, determined by using the equation (6) [122].

$$\gamma_m = \frac{\mu b \theta_m}{4\pi(1-\upsilon_p)} \quad (6)$$

Where μ is the shear modulus, b is the Burgers vector, and υ_p is the Poisson ratio. The driving pressure of a grain boundary can be obtained by summing the driving pressure of the stored deformation energy and the curvature driving pressure [123]. The latter is a function of the grain boundary curvature, K, and its surface energy, γ [124]. The grain boundary migration is a consequence of the rate theory, which estimates the boundary velocity as a function of the applied pressure [125]. The result is the general expression of V= MF [126], where M is the mobility of grain boundaries and F shows the interaction of all forces acting on the grain boundary. The grain boundary mobility can be calculated by the following equation [96]:

$$M = \begin{cases} M_m & \theta \geq 15^\circ \\ M_m\left(1-\exp\left[-5\left(\frac{\theta}{\theta_m}\right)^4\right]\right) & \theta < 15^\circ \end{cases} \quad (7)$$

Here Mm is the mobility of a HAGB. This is often calculated by the fitting method, although an exponential expression has also been proposed for it as a function of the deformation temperature [127,128].

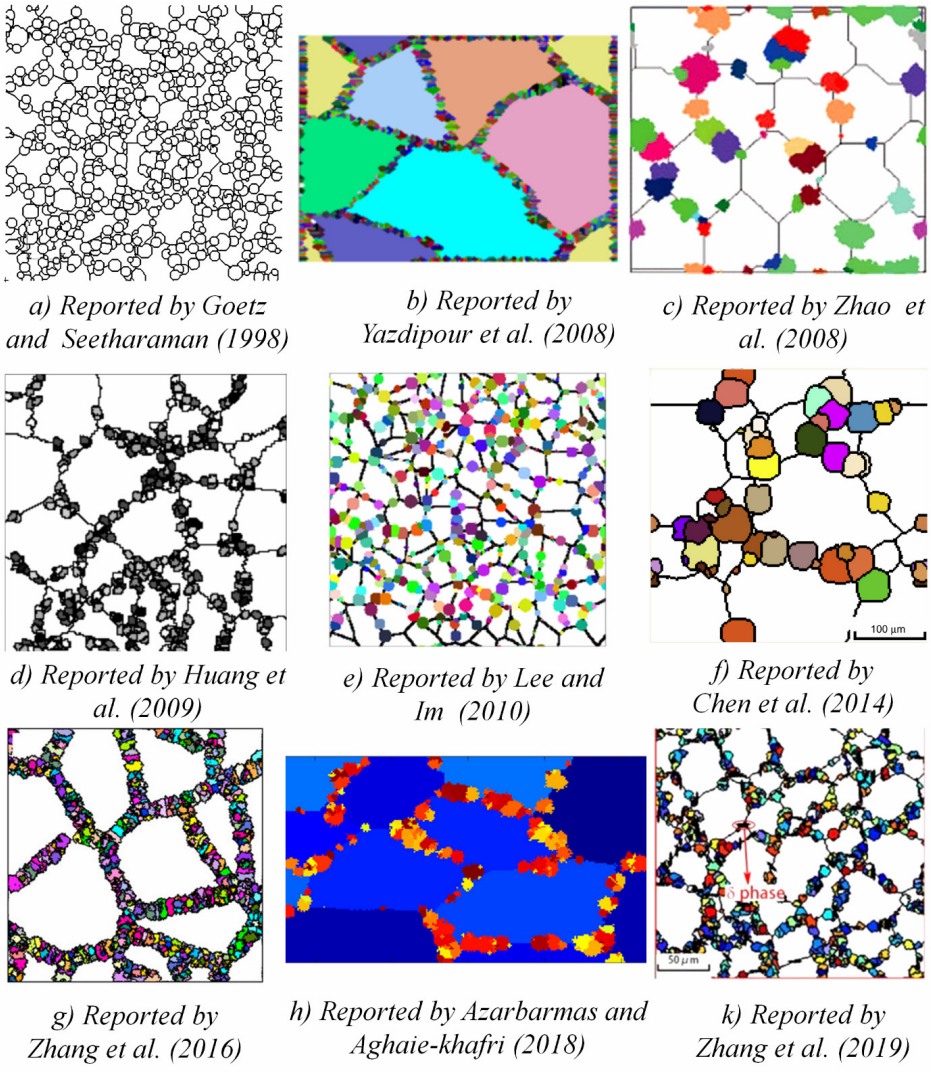

a) Reported by Goetz and Seetharaman (1998) *b) Reported by Yazdipour et al. (2008)* *c) Reported by Zhao et al. (2008)*

d) Reported by Huang et al. (2009) *e) Reported by Lee and Im (2010)* *f) Reported by Chen et al. (2014)*

g) Reported by Zhang et al. (2016) *h) Reported by Azarbarmas and Aghaie-khafri (2018)* *k) Reported by Zhang et al. (2019)*

Fig. 9. Historical trends of CA modeled two-dimensional microstructures showing the necklace structure during DDRX process, reported in a) [32], b) [111], c) [41], d) [112], e) [42], f) [113], g) [114], h) [50] and k) [115].

5.3. CA Modeling of Topological Changes

In a typical CA modeling, DRX grains are nucleated on cells belonging to grain boundaries. Accordingly, the grain boundary area and the grain topology have noticeable effects on the nucleation stage. Besides, an elongated and narrow topology of initial grains decreases the distance between growing recrystallized cells and thereby prevents them from more growth. In several published works [33, 43, 129], a uniform topology deformation procedure has been used to incorporate grain topology changes in the CA modeling of DRX, based on a vector operation, see Fig. 8b. At each strain increment, which can be extracted from FEM software, desirable topological variations are applied to the structure, and then the nucleation and growth steps of the DRX process are done by using iterations to complete the corresponding strain increment. Each point of two-dimensional space can be imagined as a vector. So a new shape is generated via the operation on each vector and making new vectors. On the other hand, the deformation itself can be displayed by a 2×2 deformation matrix in two-dimensional problems. So a uniform deformation S converts an original vector u to a new vector v:

$$v=Su \quad \text{or} \quad \begin{bmatrix} v_x \\ v_y \end{bmatrix} = \begin{bmatrix} I_x & 0 \\ 0 & I_y \end{bmatrix} \begin{bmatrix} u_x \\ u_y \end{bmatrix} \qquad (8)$$

Where u_x and u_y are the components of the original vector, while v_x and v_y are components of the new vector generated after the deformation. I_x and I_y are the ratios of final to initial lengths of unit vectors along principal axes; i.e. ln(I) will be the true strain. Because it is assumed that the volume remains constant during the deformation [14], the determinant of the deformation matrix should be unity. In the CA model, each cell can be considered as a discretized point of the space. Therefore, the geometrical position change of a cell can be calculated and imposed on its previous position according to the topology deformation model in each deformation step. It should be pointed out that the second diagonal of the deformation matrix in equation 8) is supposed to be zero. It means that there is no rotation and shear in the structure, which is not a reasonable assumption for the real deformation.

A cellular system and a material coordinate system can be used to apply topology changes [129]. Fig. 10 depicts that the material coordinate system and the corresponding grain boundary shape change with the deformation, whereas the cellular coordinate system remains constant. In this model, grain boundaries are mapped from the material coordinate system to the cellular coordinate system before the next cycle of DRX. The nucleation and growth of DRX grains occur inside the cellular coordinate system. Then, grain boundaries are mapped back to the material coordinate system for the next cycle.

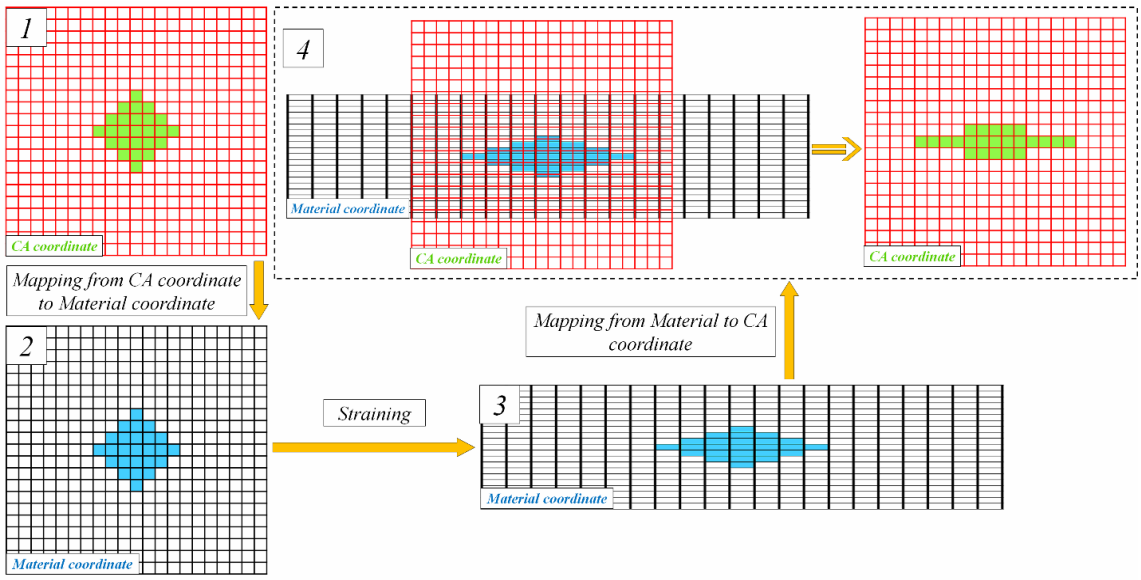

Fig. 10. A schematic of mapping a grain through the cellular and material coordinate systems for a strain step.

5.4. The Texture Evaluation

One of the main weaknesses of works done in the CA modeling of the DRX phenomenon is the lacking of a sufficient orientation definition and texture tracing. In the CA modeling, the grain boundary energy and its mobility are functions of the misorientation of two neighboring grains. So, assigning the initial orientation to grains has an important role in the nucleation and growth steps of the DRX modeling. Almost in all previous studies, initial orientations for cells were defined as a scalar number between 1-180˚ or 1-90˚, and the corresponding misorientation between two neighboring grains was assumed to be as $|\theta_1-\theta_2|$. While the crystallographic orientation of grain and the misorientation between two grains should be discussed in the real frame such as the Euler space. Another disadvantage of CA models is that they usually ignore the texture development during the deformation and its influences on the DRX nucleation and growth stages. It is well known that the nucleation and growth of a DRX grain have a severe dependency on the orientation of itself as well as surrounding grains.

The author of this study and Aghaie- Khafri [97] have proposed a CA-based model in which the initial orientations of grains have been randomly defined by using Euler angles. They have used a modified model based on Sachs's model [130] to trace the texture development during the deformation. The most important advantage of that model is its simplicity in comparison with similar models. Later, they [50] improved their model by presenting a CA model coupled with a rate-dependent (CARD) model to predict the DRX behavior of IN 718 alloy. They used a real orientation definition as three Euler angles by implementing the electron backscatter diffraction data. To determine the lattice rotation of grains, they assumed that all slip systems of grains were active during the high-temperature deformation due to the intrinsic rate dependency of the procedure.

Recently, Jaeger et al. [54], Chuan et al. [51], and Li [53] have coupled a crystal plasticity finite element model with the CA model for modeling the DRX process. Their works can be considered as a good starting point for the orientation improvement and the texture evolution in the CA modeling the DRX phenomenon. In these models, the deformation behavior of grains has been determined by using the crystal plasticity model, by recording the crystallographic slip and the rotation of the crystal lattice during the deformation [131], Fig. 8c. The rotation of the grain orientation, which is demonstrated by using a rotation tensor Q_R, can be determined as:

$$Q_R(t)=R^*(t)Q_R(t_0)[R^*(t)]^T \quad (9)$$

Where R* is the rigid rotation of the material lattice which is the result of the polar decomposition of the non-plastic deformation gradient F*:

$$F^*=R^*U^* \quad (10)$$

Where U* is the stretch tensor. Due to the importance of this issue, CA coupling with the crystal plasticity is presented as a separate section.

6. CA COUPLING WITH THE CRYSTAL PLASTICITY

The crystal plasticity-based finite element modeling (CPFEM) is increasingly utilized for the quantitative describing microstructural developments during the plastic deformation. CPFEM can estimate dislocation density increments and strain-stress fields inside grains in each step of the deformation. Moreover, the influences of the plastic deformation on grain boundaries distributions can be assessed by CPFEM. The grain boundaries distribution is a key parameter during the DRX phenomenon, especially the DDRX process in which nuclei form along the initial grain boundaries.

Regarding the physical origin of the dislocations sliding, it is possible to describe a heterogeneous deformation and trace changes of grains orientations by using the CPFEM. In this model, the dislocation density can be related to shear strains within slip systems. Owing to the constitutive nature of the crystal plasticity approach, the heterogeneous deformation and softening mechanisms can be numerically coupled by using this method. In a CA-CPFEM, the local stress and strain tensors, as well as crystals orientations and the dislocation density are calculated utilizing the crystal plasticity model, in each strain step. Then, these parameters are implemented in the CA model to evaluate the DRX transition rules. The generation of CA cells and linking them to finite

elements can be performed in a finite element based code via the user-subroutine [132]. The main parameters in a CA-CPFEM are the dislocation density and grains orientations. There are various methods for defining the grain orientation: a scalar number, three Euler angles, and the orientation matrix (see Fig. 11). Since Euler angles and orientation matrix definitions can exactly show the real orientation of a crystal, they are utilized in CA-CPFEM models.

Jaeger et al. [54] have coupled the CA modeling with the CPFEM to model the DRX behavior of Inconel 718 polycrystalline during the hot compression tests. They have considered both finite elastic distortions and large lattice rotations and showed that the model was capable to simulate developments of the dislocations density, local orientations, strain and stress fields within the grains, and average flow curves. Also, they have successfully predicted the DRX kinetic and the size of recrystallized grains. They have used a real definition for the initial orientation of grains (Fig. 12-a) and presented changes of orientations in the three-dimensional microstructure by following orientations changes during the plastic deformation (Fig. 12b and c). A similar work [49] has been reported for AZ31 sheets having the HCP structure, in which both crystallographic slip systems and deformation mechanisms based on twins have been applied.

Chuan et al. [51] combined a CA model with a CPFEM to model the DDRX behavior of IMI834 alloy during the hot deformation. Deformation parameters such as the strain and crystal orientation of each grain were determined by utilizing the CPFEM and defined as input parameters into the CA model to investigate the influence of the plastic deformation on the DDRX phenomenon. It means that this model can cover a heterogeneous strain distribution within grains, which is not possible in a conventional CA model. Fig. 13 displays heterogeneous strain distributions produced via a CPFEM.

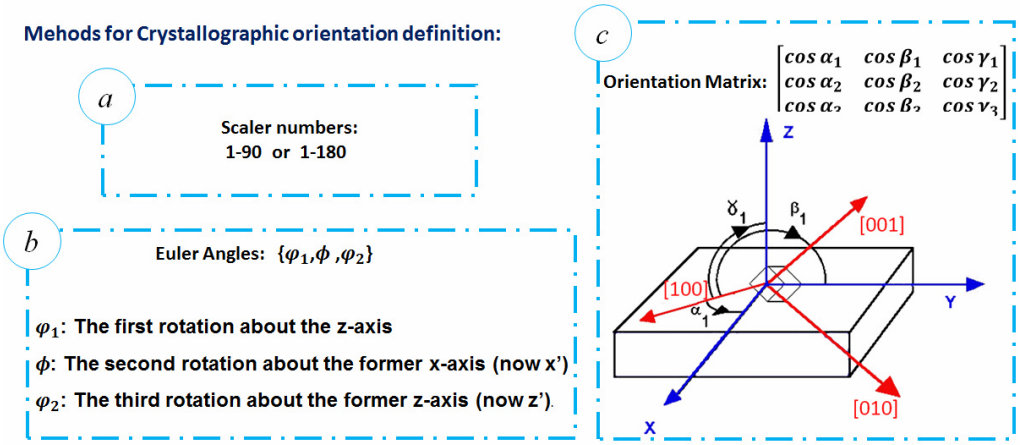

Fig. 11. Three methods to define the grain orientation; against method (a), method (b) and (c) can be used in the CA - CPFEM.

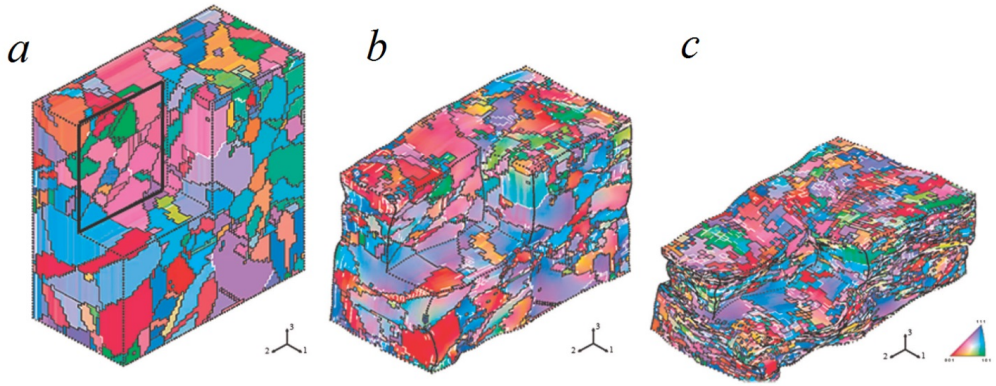

Fig. 12. Three-dimensional microstructures produced by the CA-CPFEM model for IN 718 alloy hot compressed to strains of (a) 0, (b) 0.3 and (c) 0.69 [54].

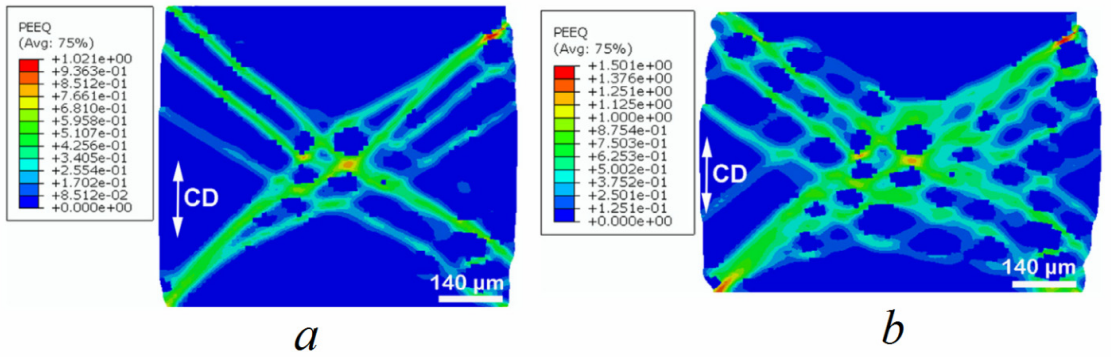

Fig. 13. The heterogeneous strain distribution of the IMI834 alloy obtained by CPFEM at 1273 K, 0.1 s^{-1} and different reductions of (a) 10% and (b) 40% [51].

Most existing CA-CPFEM models consist of three parts: i) employing CPFEM to provide the deformation data such as the dislocation density and grains orientations; ii) using the visualization method of CA to assess transition rules of DRX, and iii) illustrating the output data as morphological microstructures and average flow curves, Fig. 14.

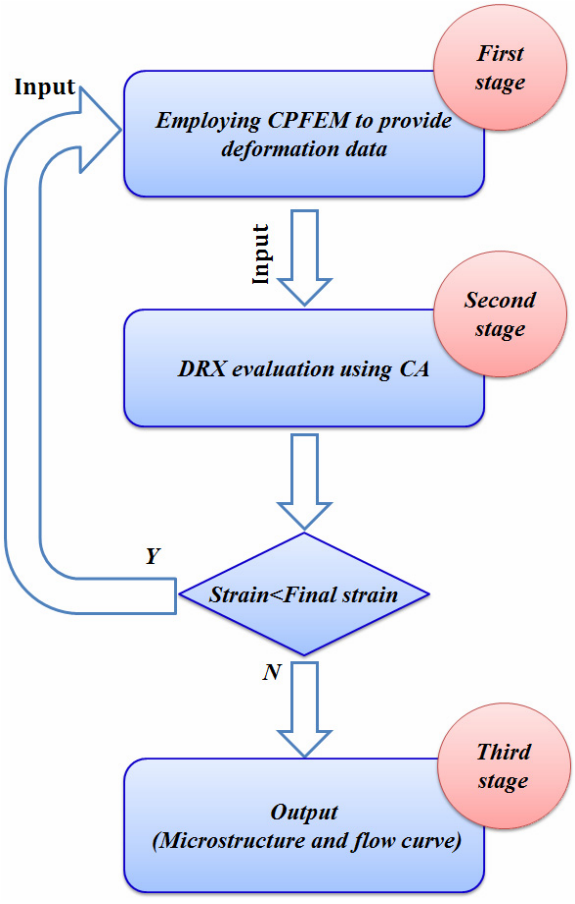

Fig. 14. Three main stages of the conventional CA-CPFEM models.

As shown in Fig. 14, the important neglected point in those works is the effect of DRX on the subsequent deformation. Recently, Li et al. [53] have presented a comprehensive CA-CPFEM model and focused on this problem. They used the CA-CPFEM modeling to couple the softening mechanisms with the heterogeneous deformation and the mechanical response during the hot deformation of TA15 alloy. The idea is that the morphological evolution of DRX can be treated as an intrinsic portion of the constitutive behavior of the material. CPFEM determines increments of heterogeneous deformation parameters (Fig. 15), which are used for the CA modeling to perform recrystallization calculations, and then the obtained DRX-experienced microstructure is returned to the CPFEM environment to calculate changes of next-step deformation parameters. These parameters are determined at levels of slip systems, single crystals, and poly-crystals. Li et al. [53] implemented these algorithms into ABAQUS/Explicit via a user material subroutine (VUMAT) platform.

As noted before, the author of this review and M. Aghaie-Khafri [50] have proposed a CA model coupled with a rate-dependent model to simulate the DRX phenomenon during the hot compression of IN 718 alloy. In this work, it has been assumed that all of the possible slip systems of polycrystalline are active during the deformation, and all of the mathematical operations were strain-based, and no stress analysis was performed. So, there is no need for implementing the model as a user subroutine into the finite element environment. Figure 16 compares the experimental data and modeling results indicating the good accuracy of the model in simulating the DRX phenomenon.

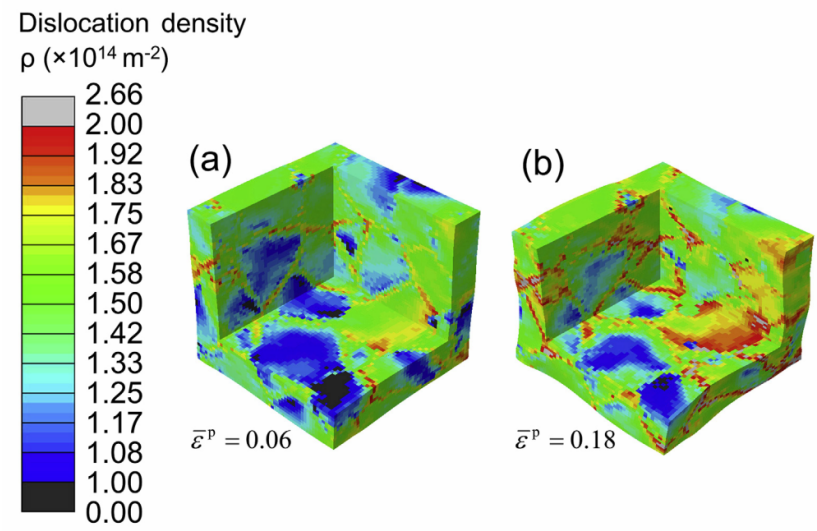

Fig. 15. CPFEM simulation results showing the dislocation density distribution at the grain level with true strains of (a) 0.06 and (b) 0.18 [53].

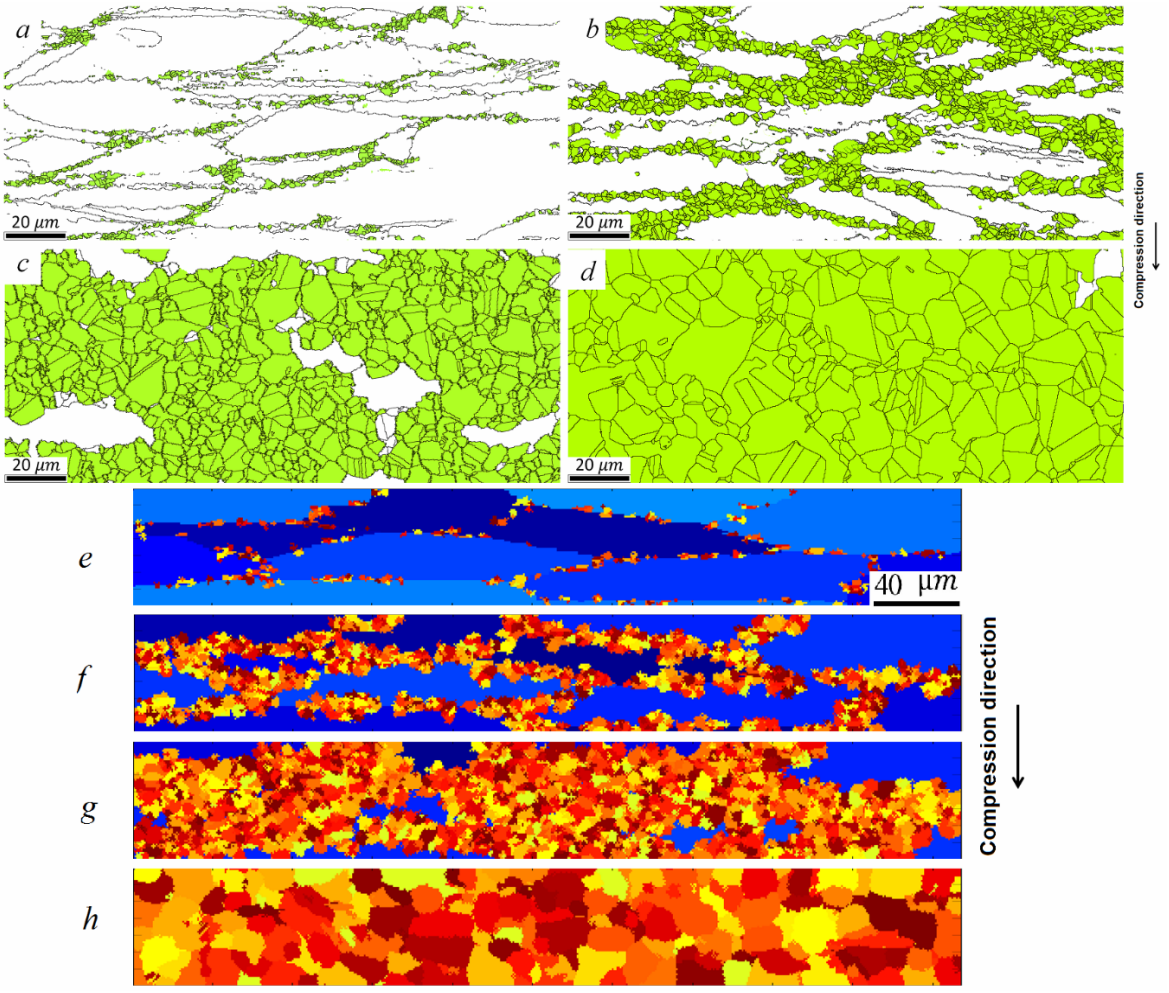

Fig. 16. The experimental data (a-d) and results of the CA model (e-f); the results are for IN 718 samples deformed at the strain rate of 0.1 s^{-1}, strain of 0.6 and temperatures of (a,e) 950, (b,f) 1000, (c,g) 1050 and (d,h) 1100 °C [50].

7. OPEN QUESTIONS

Although CA has several advantages in comparison with similar methods, see Fig. 17, there are still some issues that need to be resolved. The following sections focus on these open questions.

7.1. The High Sensitivity of CA to the Calibration

Although the calibration capability of the CA modeling is one of its advantages for simulating microstructural developments, its significant dependency on the calibration is one of the main disadvantages of it. The final produced microstructure by using the CA model is the result of comparing the predicted and real microstructures and calibrating constants values (such as C_0, M_0, etc.) to present a microstructure similar to the experimental microstructure. It means that for predicting a microstructure one should first do experiments and obtain the real microstructure and then according to experimental results calibrate CA modeling parameters for producing a microstructure. It is not a predicting method of the microstructure to decrease needs for experiments but is a process for drawing and painting experimental results. So it is necessary to lower the CA sensitivity to calibrated parameters in the future. This can be achieved by replacing constants lacking any physical meaning with physically described parameters.

7.2. Limitations in the CDRX Modeling

In a conventional CA modeling, it is assumed that the stored energy inside a grain has a homogeneous distribution. While, in real deformed microstructures, there is a strong inhomogeneity in the distribution of dislocations and dislocation cell boundaries which can form several geometrically necessary boundaries (GNBs) inside a grain. The distribution of the strain stored energy has an important role in the nucleation and growth of DRX grains. Because in the CA approach the nucleation is usually considered to occur along initial grain boundaries, it cannot model CDRX in which new DRX grains are nucleated inside interior portions of grain by the gradual transformation of LAGBs into HAGBs [133]. Considering CDRX modeling requirements, it is predictable that the real initial orientation definition and the texture development will be a necessary part of CA modeling in near future. Polycrystal plastic models can be useful to overcome the inability of strain heterogeneity modeling.

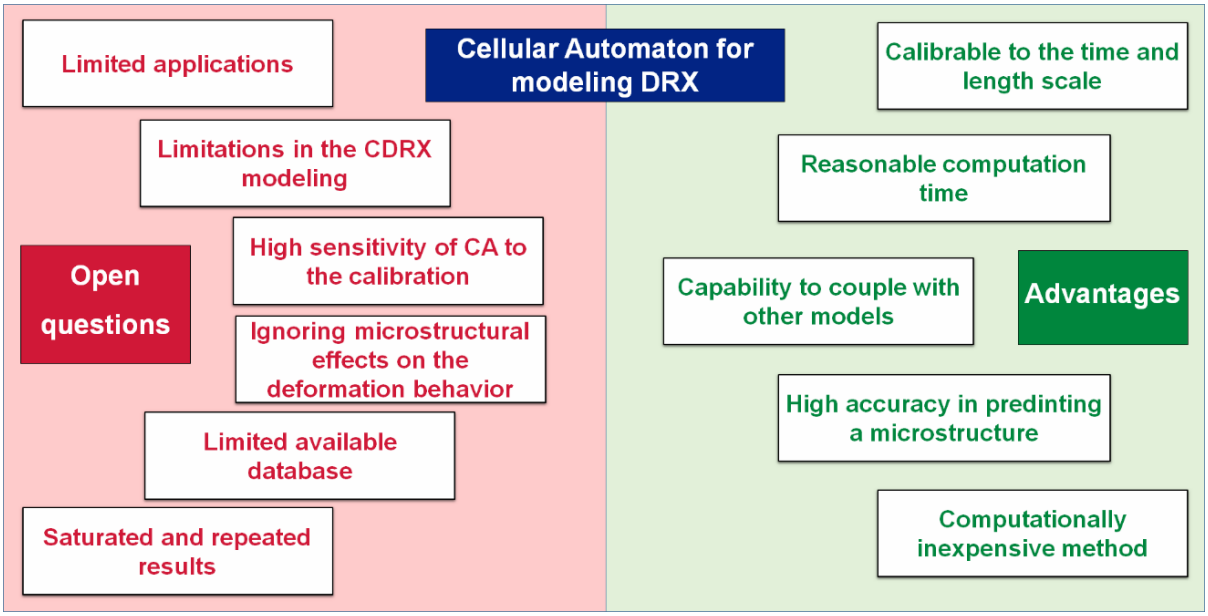

Fig. 17. The schematic showing advantages of CA for modeling DRX as well as its open questions.

7.3. Ignoring Microstructural Effects on the Deformation Behavior

Almost in all works published in the field of the CA modeling of DRX effects of deformation parameters (the strain, strain rate, deformation temperature, etc.) on the microstructural evolution have been investigated. But the influence of microstructural changes on the deformation behavior has been neglected for simplicity. Whilst the recovery and DRX can remarkably influence the stress field distribution and thereby change the obtained parameters from flow stress curves. Also, fluctuating in the mean grain size of the sample during the deformation will affect the deformation behavior. Coupling the CA method with CPFEM and using the extracted constitutive equations can solve these problems somewhat.

7.4. Limited Applications

The CA modeling has been successfully utilized to obtain a better academic understanding of fundamental aspects of microstructural phenomena. The dream of materials scientists is the construction of a CA model which can quantitatively predict the microstructure in industrial applications. During various stages of the CA modeling, a lot of assumptions are used to simplify the simulation operation which most of them are far from the real condition. These assumptions evolve the material characteristics, deformation condition, microstructural developments, the deformation mechanism, etc. Therefore, the first step to extend applications of the CA modeling is improving its simple assumptions and closing to the real condition.

7.5. Limited Available Database

In the CA modeling, transition rules define the status of cells in any time step. These rules are based on constitution equations which have several coefficients. In the available literature, there are only limited alloys with reported coefficients. On the other hand, most of the available data have been reported by approximation. Therefore, for the CA modeling of a new alloy, first of all, it is necessary to determine these parameters. Developing constitutive equations with lower coefficients and using parameters having a physical meaning can be helpful in this case.

7.6. Saturated and Repeated Results

Goetz and Seetharaman [32] were the first authors who reported a CA-based model for modeling the DRX phenomenon in 1998. Historical trends in presenting the CA modeling results of DRX can be found in Fig. 9. Although obtained microstructures have become more accurate with each passing year, it can be seen that reported results are similar to each other in the past decade. In other words, a graphical presentation of a necklace microstructure without a significant novelty in the quantitative and qualitative analysis of predictions is common in almost all of the published works in this area. The quantitative evaluation of these works is only limited to assess the size and volume fraction of recrystallized grains. In the next section, suggestions for strengthening future works are noted.

8. FUTURE PROSPECTS

8.1. Providing a Vivid Laboratory

It is interesting to observe dynamically microstructural changes during the thermomechanical processing. CA can provide a vivid laboratory to evaluate complicated and nonlinear dynamics. It may soon be within the reach that one can extend a CA model with the capability in tracking the production, migration, and annihilation of dislocations for alloys experienced the hot deformation. A developed software based on the CA method by which a user can track microstructural changes during a complicated thermomechanical process just by implementing material properties and the process condition can be an interesting achievement in this field.

8.2. Transforming from Meso to Nano-Scale Modeling

With a small bit of exaggeration, to model the DRX more realistically, CA will be transformed from the meso-scale modeling into the nano-scale modeling. In other words, the size of each cell will be a size of a molecule/atom. Therefore, against most of the published CA-based works in which only the size and distribution of grains are used for evaluating the model performance, vacancies and the dislocations density, the distribution of low and medium angle boundaries, orientation gradients and the Taylor factor distribution can be assessed to approve the quality of the model. In this case, the definition of cell grids and the neighborhood will be considered according to the crystallographic

structure of the alloy. It is clear that for nano-scale modeling of a typical microstructure consisting of several grains, a powerful computer is needed. This model could be used to control more accurately the deformation condition (such as initial treatments, the deformation temperature, strain, strain rate, and direction of loading) to obtain the required microstructure and thereby the mechanical properties. Similarly, it may be utilized for producing a material with a preferred crystallographic texture. However, to achieve such possibilities, it is necessary to overcome the challenges described in the section of "Open questions".

8.3. Online Optimizing the Performance

The accuracy of a model in predicting results is the most important parameter in a modeling procedure. So it is worth focusing on increasing the performance of the model by evaluating the accuracy. So far, the efficiency of CA models presented for modeling DRX has been checked at the end of the simulation, i.e. after completing the modeling, the accuracy of the model has been evaluated. If the accuracy was not reasonable, the simulation was repeated with some corrections until the required efficiency was obtained. This can waste a lot of time and energy. Considering this problem, it is predictable that the next-generation of CA models can check the accuracy of itself during the simulation and apply required corrections simultaneously with running. The work recently reported by Chen et al. [134] can be regarded as a promising achievement in this case. They have coupled the CA technique with "neural network-based model predictive control" methods for online optimizing the processing parameters by considering designed target microstructures.

9. CONCLUSION

The DRX phenomenon is a complex process occurring during the hot deformation which can modify the microstructure. The numerical modeling of the DRX process has become a favorite topic in industrial and scientific fields. In this paper, after a brief description of the DRX phenomenon, an overview of the CA modeling for the numerical modeling of DRX has been provided. The main conclusions of this review are summarized as follows:

1. CA modeling is a rapidly developing tool for the quantitative simulation of the DRX phenomenon during the hot deformation process.
2. In comparison with similar methods, CA is more feasible to model microstructural developments due to its ability for calibration to the time and length scale.
3. A large number of works published in this field have used very simple assumptions, and most of the lately published works are to improve these simplifications.
4. Despite the high performance of CA for modeling the DRX phenomenon, there still some challenges in this field. The calibration sensitivity, limitations in the continuous DRX modeling, neglecting microstructural effects on the deformation behavior, limited applications, and limited database as well as saturated results are the most important problems of the available literature. In this work, corresponding recommendations were suggested to overcome the aforementioned limitations.
5. Shortly, the CA modeling could be used for providing a vivid laboratory to evaluate complicated processes. Next-generation CA modeling will able to model in the nano-scale with the capability of checking and improving its accuracy during the simulation.

ACKNOWLEDGMENT

The author would like to thank A. Ghasemi and S.S. Mirjavadi for helpful discussions.

REFERENCES

1. Azimi M, Mirjavadi SS, Salandari-Rabori A., "Effect of temperature on microstructural evolution and subsequent enhancement of mechanical properties in a backward extruded magnesium alloy." Int. J. Adv. Manuf. Technol., 2018, 95, 3155–3166.
2. Zeinali M, Shafiei E, Hosseini R, Sooltanipor, R., "Hot Deformation Behavior of 17-7 PH Stainless Steel." Iran. J. Mater. Form., 2017, 4, 1–11.
3. Rappaz M., "Modeling and characterization of grain structures and defects in solidification." Curr. Opin. Solid

State Mater. Sci." 2016, 20, 37–45.
4. Bastien C, Michel D., "Cellular automata modeling of physical systems." Cell. Autom. Model. Phys. Syst., 1998, 122-137.
5. Ilachinski A., "Cellular automata: a discrete universe." World Scientific Publishing Company;, 2001, 1-52
6. Lin YC, Liu Y-X, Chen M-S, Huang, M. H., Ma, X., Long, Z. L., "Study of static recrystallization behavior in hot deformed Ni-based superalloy using cellular automaton model." Mater. Des., 2016, 99, 107–114.
7. Marx V, Reher FR, Gottstein G., "Simulation of primary recrystallization using a modified three-dimensional cellular automaton." Acta Mater., 1999, 47, 1219–1230.
8. Raabe D. "Introduction of a scalable three-dimensional cellular automaton with a probabilistic switching rule for the discrete mesoscale simulation of recrystallization phenomena." Philos. Mag. A., 1999, 79, 2339–2358.
9. Zhang F, Liu D, Yang Y, Wang, J., Zheng, Y., "Study of factors affecting simulation of static recrystallization of Ni-based superalloy through cellular automaton model." Procedia Eng., 2017, 207, 2131–2136.
10. Zhang Y, Jiang S, Hu L, Zhao, Y., & Sun, D., "Investigation of primary static recrystallization in a NiTiFe shape memory alloy subjected to cold canning compression using the coupling crystal plasticity finite element method with cellular automaton." Model. Simul. Mater. Sci. Eng., 2017, 25, 75008.
11. Zhang T, Lu S, Zhang J, Li, Z., Chen, P., Gong, H., Wu, Y., "Modeling of the static recrystallization for 7055 aluminum alloy by cellular automaton." Model. Simul. Mater. Sci. Eng., 2017, 25, 65005.
12. Afshari E, Serajzadeh S.,"Simulation of static recrystallization after cold side-pressing of low carbon steels using cellular automata." J. Mater. Eng. Perform., 2012, 21, 1553–1561.
13. Gawad J, Madej W, Kuziak R, Pietrzyk, M., "Multiscale model of dynamic recrystallization in hot rolling." Int. J. Mater. Form., 2008, 1, 69–72.
14. Shabaniverki S, Serajzadeh S., "Simulation of softening kinetics and microstructural events in aluminum alloy subjected to single and multi-pass rolling operations." Appl. Math. Model. 2016, 40, 7571–7582.
15. Chen S, Chen J., "Simulation of microstructures in solidification of aluminum twin-roll casting." Trans. Nonferrous Met. Soc. China., 2012, 22, 1452–1456.
16. Zhang L, Zhang C., "Two-dimensional cellular automaton model for simulating structural evolution of binary alloys during solidification." Trans. Nonferrous Met. Soc. China., 2006, 16, 1410–1416..
17. Tsai D, Hwang W., "Numerical simulation of solidification morphologies of Cu-0.6Cr casting alloy using modified cellular automaton model." Trans. Nonferrous Met. Soc. China . 2010, 20, 1072–1077..
18. Zhao J, Wang G-X, Ye C, Dong, Y., "Cellular automata modeling of nitriding in nanocrystalline metals." Comput. Mater. Sci. 2016, 118, 342–352..
19. di Caprio D, Stafiej J, Luciano G, Arurault, L., "3D cellular automata simulations of intra and intergranular corrosion." Corros. Sci. 2016, 112, 438–450.
20. Xiao Z, Jun H, Yuqi W, Maosheng, Z., Zaoxiao, Z., "Simulation of Pitting Corrosion for Ni-based Alloy Using a Cellular Automata Model." Rare Met. Mater. Eng. 2015, 44, 2347–2352.
21. Wang H, Han E-H., "Computational simulation of corrosion pit interactions under mechanochemical effects using a cellular automaton/finite element model." Corros. Sci. 2016, 103, 305–311.
22. Wu M, Xiong S., "Modeling of equiaxed and columnar dendritic growth of magnesium alloy." Trans. Nonferrous Met. Soc. China. 2012, 22, 2212–2219.
23. Janssens KGF, "An introductory review of cellular automata modeling of moving grain boundaries in polycrystalline materials. " Math., Comput., Simul., 2010, 80, 1361–1381.
24. Li Z, Wang J, Huang H. "A new-curvature cellular automata model of austenite grain growth." Mater. Res. Express. 2019, 6, 9, 0965b5.

25. Vertyagina Y, Marrow TJ., "3D Cellular Automata fracture model for porous graphite microstructures." Nucl. Eng. Des., 2016, 323, 202-208.
26. Pourian MH, Bridier F, Pilvin P, Bocher, P., "Prediction of crack initiation sites in alpha Ti-alloys microstructures under dwell-fatigue using Cellular Automaton simulation method." Int. J. Fatigue. 2016, 85, 85–97.
27. Rauch L, Chmura A, Gronostajski Z, Polak, S., Pietrzyk, M., "Cellular automata model for prediction of crack initiation and propagation in hot forging tools." Arch. Civ. Mech. Eng. 2016, 16, 437–447.
28. Yan F, Feng X-T, Pan P-Z, Li, S.-J.,. "Discontinuous cellular automaton method for crack growth analysis without remeshing." Appl. Math. Model. 2014, 38, 291–307.
29. Yang H, Wu C, Li H, Fan, X., "Review on cellular automata simulations of microstructure evolution during metal forming process: Grain coarsening, recrystallization and phase transformation." Sci. China Technol. Sci. 2011, 54, 2107–2118.
30. Zheng C, Raabe D., "Interaction between recrystallization and phase transformation during intercritical annealing in a cold-rolled dual-phase steel: A cellular automaton model." Acta Mater. 2013, 61, 5504–5517.
31. Song KJ, Wei YH, Fang K, Dong, Z. B., Zhan, X. H., Zheng, W. J.,, "Cellular automaton-based study of factors that affect dynamic solid phase transformation kinetics." Appl. Math. Model.2015, 39, 5058–5072.
32. Goetz RL, Seetharaman V., "Modeling dynamic recrystallization using cellular automata." Scr. Mater. 1998, 38, 405–413.
33. Xiao N, Zheng C, Li D, Li, Y., "A simulation of dynamic recrystallization by coupling a cellular automaton method with a topology deformation technique." Comput. Mater. Sci. 2008, 41, 366–374.
34. Qian M, Guo ZX., "Cellular automata simulation of microstructural evolution during dynamic recrystallization of an HY-100 steel." Mater. Sci. Eng. A. 2004, 365, 180–185.
35. Lee HW, Im Y-T., "Cellular automata modeling of grain coarsening and refinement during the dynamic recrystallization of pure copper." Mater. Trans. 2010, 51, 1614–1620.
36. Guo NN, Wang L, Luo LS, Li, X. Z., Chen, R. R., Su, Y. Q., Guo, J. J., Fu, H. Z., "Hot deformation characteristics and dynamic recrystallization of the MoNbHfZrTi refractory high-entropy alloy." Mater. Sci. Eng. A. 2015, 651, 698-707;
37. Chen XM, Lin YC, Wen DX, Zhang, J. L., He, M., "Dynamic recrystallization behavior of a typical nickel-based superalloy during hot deformation." Mater. Des. 2014, 57, 568–577.
38. Xiao LIU, Li L, He F, Jia, Z., Zhu, B., Zhang, L., "Simulation on dynamic recrystallization behavior of AZ31 magnesium alloy using cellular automaton method coupling Laasraoui–Jonas model." Trans. Nonferrous Met. Soc. China. 2013, 23, 2692–2699.
39. Zhang D, Niu W, Cao X, Liu, Z., "Effect of standard heat treatment on the microstructure and mechanical properties of selective laser melting manufactured Inconel 718 superalloy." Mater. Sci. Eng. A. 2015, 644, 32-40.
40. Reyes LA, Páramo P, Zamarripa AS, de la Garza, M., Mata, M. P. G., "Grain size modeling of a Ni-base superalloy using cellular automata algorithm." Mater. Des. 2015, 83, 301–307.
41. Zhao JW, Ding H, Zhao WJ, Cao, F. R., Hou, H. L., Li, Z. Q., "Modeling of dynamic recrystallization of Ti6Al4V alloy using a cellular automaton approach." Acta Metall. Sin. (English Lett. 2008, 21, 260–268.
42. Lee HW, Im Y-T., "Numerical modeling of dynamic recrystallization during nonisothermal hot compression by cellular automata and finite element analysis." Int. J. Mech. Sci. 2010, 52, 1277–1289.
43. Chen F, Qi K, Cui Z, Lai, X., "Modeling the dynamic recrystallization in austenitic stainless steel using cellular automaton method." Comput. Mater. Sci. 2014, 83, 331–340.

44. Li J, Xie Z, Li S, Zang, Y., "Modeling on dynamic recrystallization of aluminium alloy 7050 during hot compression based on cellular automaton." J. Cent. South Univ. 2016, 23, 497–507.
45. Chen F, Cui Z., "Modeling the Dynamic Recrystallization: A Modified Cellular Automaton Method." Proc. 6th Int. Conf. Recryst. Grain Growth (ReX&GG 2016). Springer, 2016, 57–62.
46. Sitko M, Pietrzyk M, Madej L., "Time and length scale issues in numerical modelling of dynamic recrystallization based on the multi space cellular automata method." J. Comput. Sci. 2016, 16, 98–113.
47. Chen F, Cui Z, Ou H, Long, H., "Mesoscale modeling and simulation of microstructure evolution during dynamic recrystallization of a Ni-based superalloy." Appl. Phys. A. 2016, 122, 890.
48. Haase C, Kühbach M, Barrales-Mora LA, Wong, S. L., Roters, F., Molodov, D. A., & Gottstein, G., "Recrystallization behavior of a high-manganese steel: experiments and simulations." Acta Mater. 2015, 100, 155–168.
49. Popova E, Staraselski Y, Brahme A, Mishra, R. K., Inal, K., "Coupled crystal plasticity – Probabilistic cellular automata approach to model dynamic recrystallization in magnesium alloys." Int. J. Plast.2015, 66, 85–102.
50. Azarbarmas M, Aghaie-Khafri M., "A New Cellular Automaton Method Coupled with a Rate-dependent (CARD) Model for Predicting Dynamic Recrystallization Behavior." Metall. Mater. Trans. A. 2018, 49, 1916-1930.
51. Chuan W, He Y, Wei LH., "Modeling of discontinuous dynamic recrystallization of a near-α titanium alloy imi834 during isothermal hot compression by combining a cellular automaton model with a crystal plasticity finite element method." Comput. Mater. Sci. 2013, 79, 944–959.
52. Popova E., "Crystal Plasticity Based Numerical Modelling of Dynamic Recrystallization in Magnesium Alloys." Evdokia Popova, 2015, 1-112.
53. Li H, Sun X, Yang H., "A three-dimensional cellular automata-crystal plasticity finite element model for predicting the multiscale interaction among heterogeneous deformation, DRX microstructural evolution and mechanical responses in titanium alloys." Int. J. Plast. 2016, 87, 154–180.
54. De Jaeger J, Solas D, Fandeur O, Schmitt, J.-H., Rey, C., "3D numerical modeling of dynamic recrystallization under hot working: Application to Inconel 718." Mater. Sci. Eng. A. 2015, 646, 33–44.
55. Azarbarmas M, Aghaie-Khafri M, Cabrera JM, Calvo, J., "Microstructural evolution and constitutive equations of Inconel 718 alloy under quasi-static and quasi-dynamic conditions." Mater. Des. 2016, 94, 28–38.
56. Zheng T, Li D, Zeng X, Ding, W., "Hot compressive deformation behaviors of Mg–10Gd–3Y–0.5 Zr alloy." Prog. Nat. Sci. Mater. Int. 2016, 26, 78–84.
57. Ghazani MS, Vajd A, Mosadeg B., "Prediction of Critical, Stress and Strain for the Onset of Dynamic Recrystallization in Plain Carbon Steels." Iran. J. Mater. Sci. Eng. 2015, 12, 52–58.
58. Huang K, Logé RE., "A review of dynamic recrystallization phenomena in metallic materials." Mater. Des. 2016, 111, 548–574.
59. Azarbarmas M, Aghaie-Khafri M, Cabrera JM, Calvo J., "Dynamic recrystallization mechanisms and twining evolution during hot deformation of Inconel 718." Mater. Sci. Eng. A. 2016, 678, 137–152.
60. Mirjavadi SS, Alipour M, Emamian S, Kord, S., Hamouda, A. M. S., Koppad, P. G., Keshavamurthy, R., "Influence of TiO2 nanoparticles incorporation to friction stir welded 5083 aluminum alloy on the microstructure, mechanical properties and wear resistance." J. Alloys Compd.2017, 712, 795–803.
61. Roucoules C, Hodgson PD., "Post-dynamic recrystallisation after multiple peak dynamic recrystallisation in C–Mn steels." Mater. Sci. Technol. 1995, 11, 548–556.
62. Hallberg H, Wallin M, Ristinmaa M., "Simulation of discontinuous dynamic recrystallization in pure Cu using a probabilistic cellular automaton." Comput. Mater. Sci. 2010, 49, 25–34.

63. Hajkazemi J, Zarei-Hanzaki A, Sabet M, Khoddam, S., "Double-hit compression behavior of TWIP steels." Mater. Sci. Eng. A. 2011, 530, 233–238.
64. Mirzadeh H, Najafizadeh A, Moazeny M., "Flow curve analysis of 17-4 PH stainless steel under hot compression test." Metall. Mater. Trans. A. 2009, 40, 2950–2958.
65. Gourdet S, Montheillet F., "A model of continuous dynamic recrystallization." Acta Mater. 2003, 51, 2685–2699.
66. Montheillet F, Thomas J-P., "Dynamic recrystallization of low stacking fault energy metals." Met. Mater. with High Struct. Effic. Springer, 2004, 357–368.
67. Yang Y, Peng X, Wen H, Zheng, B., Zhou, Y., Xie, W., Lavernia, E. J., "Influence of extrusion on the microstructure and mechanical behavior of Mg-9Li-3Al-xSr alloys." Metall. Mater. Trans. A. 2013, 44, 1101–1113.
68. Mirjavadi SS, Alipour M, Hamouda AMS, Matin, A., Kord, S., Afshari, B. M., Koppad, P. G., "Effect of multi-pass friction stir processing on the microstructure, mechanical and wear properties of AA5083/ZrO_2 nanocomposites." J. Alloys Compd. 2017, 726, 1262–1273.
69. Sakai T, Miura H, Goloborodko A, Sitdikov, O., "Continuous dynamic recrystallization during the transient severe deformation of aluminum alloy 7475." Acta Mater. 2009, 57, 153–162.
70. Kühbach M, Gottstein G, Barrales-Mora LA., "A statistical ensemble cellular automaton microstructure model for primary recrystallization." Acta Mater. 2016, 107, 366–376.
71. Satbhai O, Roy S, Ghosh S., "A parametric multi-scale, multiphysics numerical investigation in a casting process for Al-Si alloy and a macroscopic approach for prediction of {ECT} and {CET} events." Appl. Therm. Eng. 2017, 113, 386–412.
72. Hesselbarth HW, Göbel IR., "Simulation of recrystallization by cellular automata." Acta Metall. Mater. 1991, 39, 2135–2143.
73. Mukhopadhyay P., "Recrystallization microstructure modelling from superimposed deformed microstructure on microstructure model., Bull. Mater. Sci. 2009, 32, 415–420.
74. Barati R., "A novel approach in optimization problem for research reactors fuel plate using a synergy between cellular automata and quasi-simulated annealing methods." Ann. Nucl. Energy. 2014, 70, 56–63.
75. Raabe D., "Computational Materials Science: The Simulation of Materials Microstructures and Properties." Wiley-VCH, 1998, 201-202.
76. Athanassopoulos S, Kaklamanis C, Kalfoutzos G, Papaioannou, E., "Cellular automata: simulations using matlab." Proc. Sixth Int. Conf. Digit. Soc. 2012, 63–68.
77. Yip S., "Handbook of materials modeling." Springer Science & Business Media, 2007, 2174-2175.
78. Raabe D., "Multiscale recrystallization models for the prediction of crystallographic textures with respect to process simulation." J. Strain Anal. Eng. Des. 2007, 42, 253–268.
79. Stefanescu D., "Science and engineering of casting solidification." Springer, 2015, 274-275.
80. Raabe D., "Mesoscale simulation of recrystallization textures and microstructures." Adv. Eng. Mater. 2001, 3, 745.
81. Komplexnej B., "Cellular Automaton Technique as a Tool for a Complex Analsis of the Microstructure Evolution and Rheological Behaviour." Acta Metall. Slovaca. 2005, 11, 45–53.
82. Ghosh S, Gabane P, Bose A, Chakraborti, N., "Modeling of recrystallization in cold rolled copper using inverse cellular automata and genetic algorithms." Comput. Mater. Sci. 2009, 45, 96–103.
83. Zhi Y, Liu X, Yu H., "Cellular automaton simulation of hot deformation of TRIP steel." Comput. Mater. Sci. 2014, 81, 104–112.
84. Goins PE, Holm EA., "The Material Point Monte Carlo model: A discrete, off-lattice method for microstructural evolution simulations." Comput. Mater. Sci. 2016, 124, 411–419.
85. Hore S, Das SK, Banerjee S, Mukherjee S., "Computational modelling of static recrystallization and two dimensional microstructure evolution during hot strip rolling of advanced high strength steel." J. Manuf. Process. 2015, 17, 78–87.

86. Sepehrband P, Wang X, Jin H, Esmaeili, S.. "Microstructural evolution during non-isothermal annealing of a precipitation-hardenable aluminum alloy: Experiment and simulation." Acta Mater. 2015, 94, 111–123.
87. Liang L, Mei Z-G, Kim YS, Ye, B., Hofman, G., Anitescu, M., Yacout, A. M., "Mesoscale model for fission-induced recrystallization in U-7Mo alloy." Comput. Mater. Sci. 2016, 124, 228–237.
88. Chen L, Chen J, Lebensohn RA, Ji, Y. Z., Heo, T. W., Bhattacharyya, S., Chang, K., Mathaudhu, S., Liu, Z. K., Chen, L.-Q., "An integrated fast Fourier transform-based phase-field and crystal plasticity approach to model recrystallization of three dimensional polycrystals." Comput. Methods Appl. Mech. Eng. 2015, 285, 829–848.
89. Zhao P, Low TSE, Wang Y, Niezgoda, S. R., "An integrated full-field model of concurrent plastic deformation and microstructure evolution: Application to 3D simulation of dynamic recrystallization in polycrystalline copper." Int. J. Plast.2016, 80, 38–55.
90. Kamachali RD, Kim S-J, Steinbach I., "Texture evolution in deformed AZ31 magnesium sheets: Experiments and phase-field study." Comput. Mater. Sci.. 2015, 104, 193–199.
91. Militzer M., "Phase field modeling of microstructure evolution in steels." Curr. Opin. Solid State Mater. Sci. 2011, 15, 106–115.
92. Piękoś K, Tarasiuk J, Wierzbanowski K, Bacroix, B., K. Pie˛kos´, J. Tarasiuk, K. Wierzbanowski, B. B., "Generalized vertex model of recrystallization – Application to polycrystalline copper." Comput. Mater. Sci. 2008, 42, 584–594.
93. Piękoś K, Tarasiuk J, Wierzbanowski K, Bacroix, B., "Stochastic vertex model of recrystallization." Comput. Mater. Sci. 2008, 42, 36–42.
94. Sazo AHJ, Torres CE, Emelianenko M, Golovaty, D., "A vertex model of recrystallization with stored energy implemented in GPU." Mater. Res. Express. 2019, 6, 55506.
95. Kim D-K, Woo W, Park W-W, Im, Y.-T., Rollett, A., "Mesoscopic coupled modeling of texture formation during recrystallization considering stored energy decomposition." Comput. Mater. Sci. 2017, 129, 55–65.
96. Liu Y-X, Lin YC, Zhou Y., "2D cellular automaton simulation of hot deformation behavior in a Ni-based superalloy under varying thermal-mechanical conditions." Mater. Sci. Eng. A. 2017, 691, 88–99.
97. Azarbarmas M, Aghaie-Khafri M., "Dynamic Recrystallization and Texture Modeling of IN718 Superalloy." Model. Simul. Mater. Sci. Eng. 2017, 25, 075001.
98. Shojaeefard MH, Akbari M, Khalkhali A, Asadi, P., Parivar, A. H., "Optimization of microstructural and mechanical properties of friction stir welding using the cellular automaton and Taguchi method." Mater. Des. 2014, 64, 660–666.
99. Davies CHJ, Hong L., "The cellular automaton simulation of static recrystallization in cold-rolled AA1050." Scr. Mater. 1999, 40, 1145–1150.
100. Sieradzki L, Madej L., "A perceptive comparison of the cellular automata and Monte Carlo techniques in application to static recrystallization modeling in polycrystalline materials." Comput. Mater. Sci. 2013, 67, 156–173.
101. Hallberg H., "A modified level set approach to 2D modeling of dynamic recrystallization." Model. Simul. Mater. Sci. Eng. 2013, 21, 85012.
102. Marx V, Raabe D, Engler O, Gottstein, G., "Simulation of the Texture Evolution During Annealing of Cold Rolled Bcc and Fcc Metals Using a Cellular Automation Approach." Texture, Stress. Microstruct. 1997, 28, 211–218.
103. Mecking H, Kocks UF., "Kinetics of flow and strain-hardening." Acta Metall. 1981, 29, 1865–1875.
104. Zhou X, Zhang H, Wang G, Bai, X., Fu, Y., Zhao, J., "Simulation of microstructure evolution during hybrid deposition and micro-rolling process." J. Mater. Sci. 2016, 51, 6735–6749.
105. Ding R, Guo ZX., "Coupled quantitative simulation of microstructural evolution and plastic flow during dynamic recrystallization." Acta Mater. 2001, 49, 3163–3175.

106. Zhou G, Li Z, Li D, Peng, Y., Zurob, H. S., Wu, P., "A polycrystal plasticity based discontinuous dynamic recrystallization simulation method and its application to copper." Int. J. Plast. 2017, 91, 48-76.
107. Behera AN, Kapoor R, Paul B, Chakravartty, J. K., "Effect of strain on evolution of dynamic recrystallization in Nb-1wt% Zr-0.1 wt% C alloy at 1500 and 1600° C." Mater. Charact. 2017, 126, 135–143.
108. Azarbarmas M, Mirjavadi S.S., Ghasemi A. Hamouda AM. "A Combined Method to Model Dynamic Recrystallization Based on Cellular Automaton and a Phenomenological (CAP) Approach." Metals (Basel). 2018, 8, 923.
109. Liu Y-X, Lin YC, Li H-B, Wen, D.-X., Chen, X.-M., Chen, M.-S., "Study of dynamic recrystallization in a Ni-based superalloy by experiments and cellular automaton model." Mater. Sci. Eng. A. 2015, 626, 432–440.
110. Yu X, Chen S, Wang L., "Simulataion of recrystallization in cold worked stainless steel and its effect on chromium depletion by cellular automaton." Comput. Mater. Sci. 2009, 46, 66–72.
111. Yazdipour N, Davies CHJ, Hodgson PD., "Microstructural modeling of dynamic recrystallization using irregular cellular automata." Comput. Mater. Sci. 2008, 44, 566–576.
112. Huang S, Yi Y, Liu C., "Simulation of dynamic recrystallization for aluminium alloy 7050 using cellular automaton." J. Cent. South Univ. Technol. 2009, 16, 18–24.
113. Fei Chen ZC and JC., "Prediction of microstructural evolution during hot forging." Manuf. Rev. 2014, 1, 1–21.
114. Zhang C, Zhang L, Xu Q, Xia, Y., & Shen, W., "The kinetics and cellular automaton modeling of dynamic recrystallization behavior of a medium carbon Cr-Ni-Mo alloyed steel in hot working process." Mater. Sci. Eng. A. 2016, 678, 33–43.
115. Zhang F, Liu D, Yang Y, Wang, J., Liu, C., Zhang, Z., Wang, H., "Modelling and simulation of dynamic recrystallization for Inconel 718 in the presence of δ phase particles using a developed cellular automaton model." Model. Simul. Mater. Sci. Eng. 2019, 27, 3, 035002.
116. Zhang Y, Jiang S, Liang Y, Hu, L., "Simulation of dynamic recrystallization of NiTi shape memory alloy during hot compression deformation based on cellular automaton." Comput. Mater. Sci. 2013, 71, 124–134.
117. Yu X, Chen S, Wang L., "Simulation of recrystallization in cold worked stainless steel and its effect on chromium depletion by cellular automaton." Comput. Mater. Sci. 2009, 46, 66–72.
118. Li Z, Xu Q, Liu B., "Microstructure simulation on recrystallization of an as-cast nickel based single crystal superalloy." Comput. Mater. Sci. 2015, 107, 122–133.
119. Jin Z, Cui Z., "Investigation on dynamic recrystallization using a modified cellular automaton." Comput. Mater. Sci. 2012, 63, 249–255.
120. Hallberg H., "Approaches to modeling of recrystallization." Metals (Basel). 2011, 1, 16–48.
121. Read WT, Shockley W., "Dislocation models of crystal grain boundaries." Phys. Rev. 1950, 78, 275.
122. Asadi P, Givi MKB, Akbari M., "Simulation of dynamic recrystallization process during friction stir welding of AZ91 magnesium alloy." Int. J. Adv. Manuf. Technol. 2016, 83, 301–311.
123. Salehi MS, Serajzadeh S., "Simulation of static recrystallization in non-isothermal annealing using a coupled cellular automata and finite element model., Comput. Mater. Sci. 2012, 53, 145–152.
124. Salehi MS, Serajzadeh S., "Simulation of static softening behavior of an aluminum alloy after cold strip rolling." Comput. Mater. Sci. 2013, 69, 53–61.
125. Timoshenkov A, Warczok P, Albu M, Klarner, J., Kozeschnik, E., Bureau, R., Sommitsch, C., "Modelling the dynamic recrystallization in C–Mn micro-alloyed steel during thermo-mechanical treatment using cellular automata." Comput. Mater. Sci. 2014, 94, 85–94.
126. Bakhtiari M, Salehi MS., "Reconstruction of deformed microstructure using cellular automata method." Comput. Mater. Sci. 2018, 149, 1–13.

127. Gawad J, Pietrzyk M., "Application of CAFE multiscale model to description of microstructure development during dynamic recrystallization." Arch. Metall. Mater. 2007, 52, 257.
128. Han F, Tang B, Kou H, Cheng, L., Li, J., Feng, Y.,"Static recrystallization simulations by coupling cellular automata and crystal plasticity finite element method using a physically based model for nucleation." J. Mater. Sci. 2014, 49, 3253–3267.
129. Chen F, Cui Z, Liu J, Chen, W., Chen, S. "Mesoscale simulation of the high-temperature austenitizing and dynamic recrystallization by coupling a cellular automaton with a topology deformation technique." Mater. Sci. Eng. A. 2010, 527, 5539–5549.
130. Sachs GZ., "The plastic deformation mode of polycrystals." Z. Verein Deut. Ing. 1928, 72, 734.
131. Raabe D, Becker RC., "Coupling of a crystal plasticity finite-element model with a probabilistic cellular automaton for simulating primary static recrystallization in aluminium." Model. Simul. Mater. Sci. Eng. 2000, 8, 445.
132. Valvi SR, Krishnan A, Das S, Narayanan, R. G. , "Prediction of microstructural features and forming of friction stir welded sheets using cellular automata finite element (CAFE) approach." Int. J. Mater. Form. 2016, 9, 115–129.
133. Liu W, Ma Y, Zhang Y, Fan, X., Xu, C., Zhang, J., "Two dynamic recrystallization processes in a high-performance extruded Mg 94.5 Y 2 Gd 1 Zn 2 Mn 0.5 alloy." Mater. Sci. Eng. A. 2017, 690, 132–136.
134. Chen D-D, Lin YC, Wu F., "A design framework for optimizing forming processing parameters based on matrix cellular automaton and neural network-based model predictive control methods." Appl. Math. Model. 2019, 76, 918–937.
135. Kugler G, Turk R., "Modeling the dynamic recrystallization under multi-stage hot deformation." Acta Mater. 2004, 52, 4659–4668.
136. Sitko M, Madej Ł, Pietrzyk M., "Validation of cellular automata model of dynamic recrystallization." Key Eng. Mater. Trans Tech Publ, 2015, 581–586.
137. Asadi P, Givi MKB, Akbari M., "Microstructural simulation of friction stir welding using a cellular automaton method: a microstructure prediction of AZ91 magnesium alloy." Int. J. Mech. Mater. Eng. 2015, 10, 20.
138. Deng XH, Ju DY, Hu XD, Zhao, H. Y.,"Modeling of dynamic recrystallization process in AZ31 magnesium alloy using cellular automaton method." Mater. Sci. Forum. Trans Tech Publ, 2015, 19–22.
139. Yazdipour N, Dehghan-Manshadi A, Davies C, Hodgson, P. D., "Simulation of dynamic recrystallization using irregular cellular automata." Mater. forum. Institute of Materials Engineering Australasia, 2007, 164–176.
140. Sitko M, Smyk G, Madej L, Pietrzyk, M., "Development of multi-mesh Cellular Automata-Finite Element model of dynamic recrystallization during rolling process, COMPLAS, Barcelona, Spain, 2015.
141. Han F, Chen R, Yang C, Li, X., Wang, D., "Cellular Automata Simulation on Dynamic Recrystallization of TA16 Alloy during Hot Deformation." Mater. Sci. Forum. 2016, 849, 245-250.
142. Haipeng J, Lige Z, Jing L, Taiyong, W., "Cellular Automaton Modeling of Dynamic Recrystallisation Microstructure Evolution for 316LN Stainless Steel." Key Eng. Mater. 2016, 693, 548–553.
143. Jin Z-Y, Juan L, Cui Z-S, Wei, D. L., "Identification of nucleation parameter for cellular automaton model of dynamic recrystallization." Trans. Nonferrous Met. Soc. China. 2010, 20, 458–464.
144. Akbari M, Asadi P, Givi MB, Zolghadr, P., "A cellular automaton model for microstructural simulation of friction stir welded AZ91 magnesium alloy." Model. Simul. Mater. Sci. Eng. 2016, 24, 35012.
145. Ji HP, Zhang LG, Liu J, Wang, T. Y., "Microstructure Prediction of 316LN Stainless Steel for Dynamic Recrystallization Based on Cellular Automata." Key Eng. Mater. Trans Tech Publ, 2016, 674–679.
146. Huang S, Yi Y, Li P, He, H., "Simulation of dynamic recrystallization in $23Co_{13}Ni_{11}Cr_3Mo$ steel using a modified cellular automaton." J. Cent. South Univ. 2014, 21, 454–459.

147. Wang Y, Peng J, Zhong L, Pan, F., "Modeling and application of constitutive model considering the compensation of strain during hot deformation." J. Alloys Compd. 2016, 681, 455–470.
148. Sitko M, Madej Ł., "Modelling of the cellular automata space deformation within the RCAFE framework." AIP Conf. Proc. AIP Publishing, 2016, 160004.
149. Legwand A, Sitko M, Perzyński K., "RCAFE Based Numerical Model of Dynamic Recrystallization." J. Mach. Eng. 2016, 16, 52–60.
150. Ma X, Zheng C-W, Zhang X-G, Li, D.-Z.,"Microstructural Depictions of Austenite Dynamic Recrystallization in a Low-Carbon Steel: A Cellular Automaton Model." Acta Metall. Sin. (English Lett.) 2016, 29, 1127–1135.
151. Madej L, Sitko M, Legwand A, Perzynski, K., Michalik, K., "Development and evaluation of data transfer protocols in the fully coupled random cellular automata finite element model of dynamic recrystallization." J. Comput. Sci. 2018, 26, 66–77.
152. Li X, Li X, Zhou H, Zhou, X., Li, F., Liu, Q., "Simulation of dynamic recrystallization in AZ80 magnesium alloy using cellular automaton." Comput. Mater. Sci. 2017, 140, 95–104.
153. Xu Q, Zhang C, Zhang L, Shen, W., Yang, Q., "Cellular Automaton Modeling of Dynamic Recrystallization of Nimonic 80A Superalloy Based on Inhomogeneous Distribution of Dislocations Inside Grains." J. Mater. Eng. Perform. 2018, 27, 4955–4967.
154. Guan XJ, Yu BJ., "Cellular Automaton Simulation for the Effects of Uneven Distribution of Dislocation Density and Small-Sized Precipitated Particles on Dynamic Recrystallization." IOP Conf. Ser. Mater. Sci. Eng. IOP Publishing, 2017, 12025.
155. Guo Y-N, Li Y-T, Tian W-Y, Qi, H.-P., & Yan, H.-H., "Combined Cellular Automaton Model for Dynamic Recrystallization Evolution of 42CrMo Cast Steel." Chinese J. Mech. Eng. 2018, 31, 1–11.
156. Lou YP, Chen M, Li JF, Hu, X. D.,"Study on the Recrystallization of Deformation Microstructure of AZ31 Magnesium Alloy. Solid State Phenom." Trans Tech Publ, 2017, 55–58.
157. Duan C, Zhang F, Qin S, Sun, W., Wang, M., "Modeling of dynamic recrystallization in white layer in dry hard cutting by finite element—cellular automaton method." J. Mech. Sci. Technol. 2018, 32, 4299–4312.
158. Wang Z, Wang L, Gao S., "Simulation of microstructure evolution of AZ31 magnesium alloy during indenten-flatten compound deformation technology based on cellular automata." Int. J. Simul. Process Model. 2017, 12, 446–455.
159. Li L, Wang L., "Simulation of Dynamic Recrystallization Behavior under Hot Isothermal Compressions for as-extruded 3Cr20Ni10W2 Heat-Resistant Alloy by Cellular Automaton Model." High Temp. Mater. Process. 2018, 37, 635–647.
160. Chen M-S, Yuan W-Q, Lin YC, Li, H. B., Zou, Z. H., "Modeling and simulation of dynamic recrystallization behavior for 42CrMo steel by an extended cellular automaton method." Vacuum. 2017, 146, 142–151.
161. Yang S-Y, Kim J-H., "Cellular automaton calculation for dynamic recrystallization." J. Phys. Conf. Ser. IOP Publishing, 2018, 1–7.
162. Quan G, Zhang K, An C, Qiu, H., Xia, Y., "Analysis of dynamic recrystallization behaviors in resistance heating compressions of heat-resistant alloy by multi-field and multi-scale coupling method." Comput. Mater. Sci. 2018, 149, 73–83.
163. Cao Z, Sun Y, Zhou C, Wan, Z., Yang, W., Ren, L., Hu, L.,"Cellular automaton simulation of dynamic recrystallization behavior in V-10Cr-5Ti alloy under hot deformation conditions." Trans. Nonferrous Met. Soc. China., 2019, 29, 98–111.
164. Zhang T, Lu S, Wu Y, Hai, G., Optimization of deformation parameters of dynamic recrystallization for 7055 aluminum alloy by cellular automaton. Trans. Nonferrous Met. Soc. China., 2017, 27, 1327–1337.
165. Zhang H, Wang J, Chen Q, Shu, D., Wang, C., Chen, G., Zhao, Z., "Study of dynamic recrystallization behavior of T2 copper in hot working conditions by experiments and cellular automaton method." J. Alloys Compd., 2019, 784, 1071–1083.

166. Xu W, Yuan R, Wu H, Zhong, X., Guo, B., Shan, D., "Study on the dynamic recrystallization behavior of Ti-55 titanium alloy during hot compression based on Cellular Automaton model method." Procedia Eng., 2017, 207, 2119–2124.
167. Chen M-S, Yuan W-Q, Li H-B, Zou, Z.-H."Modeling and simulation of dynamic recrystallization behaviors of magnesium alloy AZ31B using cellular automaton method." Comput. Mater. Sci., 2017, 136, 163–172.
168. Zhang J, Li Z, Wen K, Huang, S., Li, X., Yan, H., Yan, L., Liu, H., Zhang, Y., Xiong, B., "Simulation of dynamic recrystallization for an Al-Zn-Mg-Cu alloy using cellular automaton". Prog. Nat. Sci. Mater. Int. 2019, 29, 4, 477-484.
169. Wang L, Fang G, Qian L. Modeling of dynamic recrystallization of magnesium alloy using cellular automata considering initial topology of grains. Mater. Sci. Eng. A., 2018, 711, 268–283.
170. Zhang C, Tang X, Zhang L, Cui, Y., "Cellular automaton modeling of dynamic recrystallization of Ni–Cr–Mo-based C276 superalloy during hot compression." J. Mater. Res., 2019, 1–11.
171. Wang Y, Xing X, Zhang Y, Jiang S.,"Investigation of the Dynamic Recrystallization of FeMnSiCrNi Shape Memory Alloy under Hot Compression Based on Cellular Automaton." Metals (Basel)., 2019, 9, 1–13.
172. Samanta A, Shen N, Ji H, Wang, W., Li, J., Ding, H., "Cellular Automaton Simulation of Microstructure Evolution for Friction Stir Blind Riveting." J. Manuf. Sci. Eng., 2018, 140, 31016.
173. Wu C, Jia B, Han S. Coupling a Cellular Automaton Model with a Finite Element Model for Simulating Deformation and Recrystallization of a Low-Carbon Micro-alloyed Steel during Hot Compression. J. Mater. Eng. Perform., 2019, 28, 938–955.
174. Chen F, Cui Z, Liu J, Zhang, X., Chen, W., "Modeling and simulation on dynamic recrystallization of 30Cr2Ni4MoV rotor steel using the cellular automaton method." Model. Simul. Mater. Sci. Eng., 2009, 17, 75015.
175. Sun F, Zhang DQ, Cheng L, Zheng, P., Liao, D. M., Zhu, B., "Microstructure Evolution Modeling and Simulation for Dynamic Recrystallization of Cr12MoV Die Steel During Hot Compression Based on Real Metallographic Image., "Met. Mater. Int., 2019, 25, 966–981.